

PUCRS

FACULDADE DE BIOCÊNCIAS
PROGRAMA DE PÓS-GRADUAÇÃO
DOUTORADO EM BIOLOGIA CELULAR E MOLECULAR

ELISA FELLER GONÇALVES DA SILVA

**AVALIAÇÃO DA ATIVIDADE ANTIFIBRÓTICA E ANTINEOPLÁSICA HEPÁTICAS DO
COMPOSTO CPBMF65, INIBIDOR DA ENZIMA URIDINA FOSFORILASE 1 HUMANA: UM
ESTUDO *IN VITRO* E *IN VIVO***

Porto Alegre
2019

PÓS-GRADUAÇÃO - *STRICTO SENSU*



Pontifícia Universidade Católica
do Rio Grande do Sul

PONTIFÍCIA UNIVERSIDADE CATÓLICA DO RIO GRANDE DO SUL
FACULDADE DE BIOCÊNCIAS
PROGRAMA DE PÓS-GRADUAÇÃO DOUTORADO EM BIOLOGIA CELULAR E
MOLECULAR

ELISA FELLER GONÇALVES DA SILVA

**AVALIAÇÃO DA ATIVIDADE ANTIFIBRÓTICA E ANTINEOPLÁSICA HEPÁTICAS
DO COMPOSTO CPBMF65, INIBIDOR DA ENZIMA URIDINA FOSFORILASE 1
HUMANA: UM ESTUDO *IN VITRO* E *IN VIVO***

Porto Alegre

2019

Ficha Catalográfica

S586a Silva, Elisa Feller Gonçalves da

Avaliação da atividade antifibrótica e antineoplásica hepáticas do composto CPBMF65, inibidor da enzima uridina fosforilase 1 humana : um estudo in vitro e in vivo / Elisa Feller Gonçalves da Silva . – 2019.

71.

Tese (Doutorado) – Programa de Pós-Graduação em Biologia Celular e Molecular, PUCRS.

Orientador: Prof. Dr. Jarbas Rodrigues de Oliveira.

Co-orientador: Prof. Dr. Pablo Machado.

1. fibrose hepática. 2. carcinoma hepatocelular. 3. enzima uridina fosforilase 1 humana (UPP1). 4. células estreladas hepáticas (GRX). 5. células de hepatocarcinoma humano (HepG2). I. Oliveira, Jarbas Rodrigues de. II. Machado, Pablo. III. Título.

Elaborada pelo Sistema de Geração Automática de Ficha Catalográfica da PUCRS
com os dados fornecidos pelo(a) autor(a).

Bibliotecária responsável: Salete Maria Sartori CRB-10/1363

ELISA FELLER GONÇALVES DA SILVA

**AVALIAÇÃO DA ATIVIDADE ANTIFIBRÓTICA E ANTINEOPLÁSICA HEPÁTICAS
DO COMPOSTO CPBMF65, INIBIDOR DA ENZIMA URIDINA FOSFORILASE 1
HUMANA: UM ESTUDO *IN VITRO* E *IN VIVO***

Tese apresentada como requisito para
obtenção do grau de Doutor pelo Programa
de Pós-Graduação em Biologia Celular e
Molecular da Faculdade de Biociências da
Pontifícia Universidade Católica do Rio
Grande do Sul

Orientador: Prof. Dr. Jarbas Rodrigues de
Oliveira

Co-orientador: Prof. Dr. Pablo Machado

Porto Alegre

2019

ELISA FELLER GONÇALVES DA SILVA

Tese apresentada como requisito para
obtenção do grau de Doutor pelo Programa
de Pós-Graduação em Biologia Celular e
Molecular da Faculdade de Biociências da
Pontifícia Universidade Católica do Rio
Grande do Sul

Aprovada em: _____ de _____ de _____.

BANCA EXAMINADORA:

Prof. Dr. Adroaldo Lunardelli – UNIRITTER

Dr. Carlos Oscar Kieling – HCPA

Prof. Dra. Rosane Souza da Silva – PUCRS

Porto Alegre

2019

AGRADECIMENTOS

Em primeiro lugar, vou sempre agradecer ao meu orientador Jarbas, que foi meu paraninfo na graduação, sem dúvida o professor que mais admirei desde o início da faculdade, e como ele mesmo diz, “tem que ter um pouco de sorte nesta vida”, tive a grande honra e uma tremenda sorte de tê-lo como orientador durante mestrado e doutorado.

Em segundo lugar, aos meus colegas de laboratório, todos tiveram um grande papel durante este percurso e um lugar no meu coração, sem eles nada seria. Porém, devo destacar os meus maiores anjos durante este tempo, a Kelly Goulart Lima e a Bruna Pasqualotto Costa que, sem dúvida, foram minhas principais incentivadoras e as que mais contribuíram para que este trabalho acontecesse tanto com ajudas técnicas como de amizade. Nunca vou esquecer de vocês.

Para encerrar, um agradecimento especial a minha família, principalmente ao meu marido Rafael, que me incentiva desde o início desta caminhada e a minha linda filha Alice que nasceu durante este período, tornando este processo mais difícil, mas ao mesmo tempo muito mais compensador.

“Somos anjos de uma só asa, e só podemos voar quando abraçados uns aos outros.”

Luciano de Crescenzo

RESUMO

A fibrose hepática, que já foi considerada como sendo meramente o acúmulo de tecido cicatricial, atualmente é reconhecida como sendo um processo dinâmico que pode progredir ao longo do tempo. Porém, embora potencialmente reversível durante os estágios iniciais, um número significativo de pacientes evolui para fibrose avançada e cirrose terminal, aumentando o risco de carcinoma hepatocelular (HCC). A busca por novos tratamentos com rotas metabólicas como alvos moleculares definidos, torna-se evidente e dentre estas rotas está a via de salvamento das pirimidinas, envolvida no metabolismo de nucleotídeos, precursores de DNA e RNA. A enzima uridina fosforilase 1 humana (UPP1) tem importante papel nesta via, sendo responsável pela concentração homeostática de uridina (Urd). A nova molécula sintética CPBMF65, inibidora da enzima UPP1, já demonstrou seu efeito biológico diminuindo os efeitos adversos causados pelo quimioterápico 5-fluorouracil (5-FU). Os níveis de Urd estão reduzidos em doenças hepáticas crônicas e a expressão de UPP1 está aumentada em tumores, quando comparados aos tecidos normais. Além disso, foi demonstrado que a Urd inibe a inflamação e a fibrose na lesão pulmonar induzida pela bleomicina, diminuindo a produção de colágeno. Por estes motivos, acreditamos que o composto CPBMF65 possa demonstrar efeitos sobre a proliferação de células estreladas hepáticas (GRX) e células de hepatocarcinoma humano (HepG2), além de exercer um efeito protetor sobre a fibrose hepática induzida por tetracloreto de carbono (CCl₄) em camundongos C57BL/6. Neste trabalho, demonstramos que o composto CPBMF65 provocou a diminuição da proliferação celular nas linhagens GRX e HepG2 sem induzir citotoxicidade. Células GRX apresentaram parada do ciclo celular, aumento significativo do percentual de células senescentes, aumento de lipídios e diminuição da contração celular. As células HepG2 também apresentaram diminuição da proliferação e tiveram similar aumento de células senescentes. Além disso, o composto em estudo demonstrou manter o efeito antiproliferativo nas células HepG2 durante o tratamento prolongado. Camundongos C57BL/6 tratados simultaneamente com CCl₄ e a molécula em estudo, tiveram diminuição significativa de ALT, apresentando propriedades anti-inflamatórias e anti-fibróticas e diminuição formação de colágeno I e α -SMA. Considerando seus efeitos hepatoprotetores, CPBMF65 pode ser considerado um potencial agente para tratamento tanto de fibrose como de hepatocarcinoma.

ABSTRACT

Hepatic fibrosis, which was once considered to be merely the accumulation of scar tissue, is now recognized as being a dynamic process that can progress over time. However, although potentially reversible during the early stages, a significant number of patients progress to advanced fibrosis and terminal cirrhosis, increasing the risk of hepatocellular carcinoma (HCC). The search for new treatments with metabolic routes as defined molecular targets becomes evident and among the routes is the salvage pathway of pyrimidines, involved in the metabolism of nucleotides, precursors of DNA and RNA. The human uridine phosphorylase 1 (UPP1) enzyme plays an important role in this pathway, being responsible for the homeostatic concentration of uridine (Urd). The new synthetic molecule CPBMF65, inhibitor of UPP1 enzyme, has already demonstrated its biological effect by reducing the adverse effects caused by the chemotherapeutic 5-fluorouracil (5-FU). Urd levels are reduced in chronic liver diseases and UPP1 expression is increased in tumors when compared to normal tissues. In addition, Urd has been shown to inhibit inflammation and fibrosis in bleomycin-induced lung injury, decreasing collagen production. For these reasons, we believe that the compound CPBMF65 can demonstrate effects on the proliferation of hepatic stellate cells (GRX) and human hepatocarcinoma cells (HepG2), in addition to exerting a protective effect on hepatic fibrosis induced by carbon tetrachloride (CCl₄) in mice C57BL/6. In this work, we demonstrated that the compound CPBMF65 caused the decrease of the cellular proliferation in the GRX and HepG2 lines without inducing cytotoxicity. GRX cells presented cell cycle arrest, significant increase in the percentage of senescent cells, increase of lipids droplets and decrease of cellular contraction. HepG2 cells also showed decreased proliferation and had similar increase of senescent cells. In addition, the subject compound has been shown to maintain the antiproliferative effect on HepG2 cells during prolonged treatment. C57BL/6 mice treated simultaneously with CCl₄ and the molecule under study, had significant decrease of ALT, exhibiting anti-inflammatory and anti-fibrotic properties and decreased formation of collagen I and α -SMA. Considering its hepatoprotective effects, CPBMF65 can be considered a potential agent for treatment of both fibrosis and hepatocarcinoma.

SUMÁRIO

CAPÍTULO 1

1. INTRODUÇÃO	9
1.1. FIBROSE E CÉLULAS ESTRELADAS HEPÁTICAS	9
1.2. HEPATOCARCINOMA E CÉLULAS HEPG2	10
1.3. FIBROSE, HEPATOCARCINOMA E TERAPIAS DISPONÍVEIS.....	11
1.4. CPBMF65 E O PAPEL DA URIDINA NAS DOENÇAS HEPÁTICAS E NO CÂNCER.....	12
2. JUSTIFICATIVA	13
3. OBJETIVOS	14
3.1. OBJETIVO GERAL	14
3.2. OBJETIVOS ESPECÍFICOS	14
3.2.1. AVALIAÇÃO DO EFEITO ANTIFIBRÓTICO HEPÁTICO <i>IN VITRO</i> E <i>IN VIVO</i>	14
3.2.2. AVALIAÇÃO DO EFEITO ANTINEOPLÁSICO HEPÁTICO <i>IN VITRO</i>	15

CAPÍTULO 2

Manuscrito submetido para o periódico *European Journal Pharmacology*

“Therapeutic effect of Uridine phosphorylase 1 (UPP1) inhibitor on activated hepatic stellate cells and on carbon tetrachloride-induced liver fibrosis in mice”	18
---	-----------

CAPÍTULO 3

Manuscrito submetido para o periódico *Toxicology in Vitro*

“Uridine phosphorylase 1 (UPP1) inhibitor reduces HepG2 cell proliferation through cell cycle arrest and senescence”	40
--	-----------

CAPÍTULO 4

CONSIDERAÇÕES FINAIS	65
REFERÊNCIAS	68
ANEXO- Carta da Comissão de Ética para o Uso de Animais	71

Capítulo 1

1. INTRODUÇÃO

1.1. FIBROSE E CÉLULAS ESTRELADAS HEPÁTICAS

1.2. HEPATOCARCINOMA E CÉLULAS HEPG2

1.3. FIBROSE, HEPATOCARCINOMA E TERAPIAS DISPONÍVEIS

1.4. CPBMF65

1.5. PAPEL DA URIDINA NAS DOENÇAS HEPÁTICAS E NO
CANCÊR

2. JUSTIFICATIVA

3. OBJETIVOS

3.1. OBJETIVO GERAL

3.2. OBJETIVOS ESPECÍFICOS

1. INTRODUÇÃO

1.1. FIBROSE E CÉLULAS ESTRELADAS HEPÁTICAS

Fibrose é uma resposta cicatricial que ocorre em pacientes com lesão hepática crônica e é caracterizada por um aumento do depósito de componentes de matriz extracelular (ECM), como colágeno, elastina laminina e fibronectina (1). O dano crônico causado por drogas, desordens metabólicas, ataque imune ou infecção é requerido para o acúmulo da fibrose. A cirrose é o estágio mais avançado da fibrose e se caracteriza pela distorção do parênquima hepático com formação de nódulos e septos, fluxo sanguíneo alterado e, principalmente, o risco de insuficiência hepática (2). As células estreladas hepáticas (HSC), quando ativadas, são as maiores produtoras de componentes de ECM e, por isso, acredita-se que sejam as principais células envolvidas no processo fibrótico. Essas células podem ser encontradas em dois estágios fenotípicos diferentes: quiescente e ativadas. As HSC quiescentes acumulam retinol (vitamina A) nas gotículas lipídicas de seu citoplasma, contribuindo para a arquitetura tridimensional do fígado e para a síntese de proteínas que vão formar e degradar a ECM (3). Já, quando ativadas, essas células perdem a capacidade de armazenar retinol, alteram a composição e aumentam a síntese dos componentes de ECM, como desmina, alfa actina de músculo liso (α -SMA) e colágeno tipo I. O colágeno tipo I é o principal componente de ECM liberado quando HSC estão ativadas e sua produção é característica desse fenótipo celular (4).

A linhagem celular murina (GRX) foi obtida a partir de granulomas fibróticos induzidos em fígado de camundongos C3N/HeN por infecção experimental com *Schistosoma mansoni*. É considerada a mais antiga linhagem representativa das células do tecido conjuntivo do fígado, apresenta morfologia semelhante aos miofibroblastos e secreta colágeno tipo I e III (5). Estas células possuem propriedades pró-inflamatórias e pró-fibrogênicas (fenótipo ativado), porém, existem vários agentes químicos (N-acetilcisteína (NAC)) e biológicos (extrato da pimenta dedo-de-moça) que podem induzir a sua reversão para o fenótipo quiescente, modificando o seu metabolismo lipídico (6).

1.2. HEPATOCARCINOMA E CÉLULAS HEPG2

O carcinoma hepatocelular (HCC) é o tipo de tumor mais prevalente entre os tumores primários que atingem o fígado (7). O HCC é o sexto câncer mais comum e a segunda causa de morte relacionada ao câncer no mundo, tendo sua incidência triplicada nos Estados Unidos nas últimas três décadas (8). Está mais presente em populações asiáticas, o que pode ocorrer devido a maior frequência de polimorfismo genético no fator de necrose tumoral alfa (TNF- α), uma das principais citocinas pró-inflamatórias ligada ao HCC (9). O HCC é uma doença silenciosa, normalmente detectada em estágio avançado, o que diminui a taxa de sobrevivência para aproximadamente 14% dentro de um período de cinco anos (10). O seu desenvolvimento geralmente está relacionado a uma doença hepática crônica, que pode ser originada por uma infecção viral (hepatite B e C), alcoolismo, doenças biliares e hemocromatose primária (11, 12). Alguns estudos sugerem que pacientes com doença hepática não alcoólica (NAFLD, *non-alcoholic fatty liver disease*) têm mais risco de desenvolver HCC, tornando a obesidade e o diabetes mellitus potenciais fatores de risco para HCC (8). Trabalhos recentes também forneceram evidências de que a *Helicobacter pylori* (*H. pylori*), uma bactéria gram-negativa, pode estar envolvida na patogênese de algumas doenças do fígado, inclusive no HCC.

Outro fator associado ao desenvolvimento de HCC são as aflotoxinas, metabólitos provenientes dos fungos *Aspergillus flavus* e *Aspergillus parasiticus*, contaminantes frequentes em uma série de alimentos básicos, como cereais, com prevalência em comunidades de clima tropical e sub-tropical, principalmente na África subsaariana, Ásia Oriental e partes da América do Sul. A contaminação ocorre durante o crescimento dos grãos e como resultado de armazenamento deficiente em instalações inapropriadas (13, 14).

A HepG2 é uma linhagem celular derivada do tecido do fígado de um homem americano caucasiano de 15 anos de idade, com células bem diferenciadas de hepatocarcinoma (15). Estas células são de fácil manuseio, sendo cultivadas com sucesso em grande escala e utilizadas como modelo de tumores de células hepáticas, visto que mantêm funções metabólicas semelhantes aos hepatócitos (16). A linhagem HepG2 é derivada de carcinoma hepatocelular, apresenta morfologia

epitelial, crescimento aderente e não é tumorigênica em camundongos imunossuprimidos (15).

1.3. FIBROSE, HEPATOCARCINOMA E TERAPIAS DISPONÍVEIS

Tradicionalmente, o tratamento da fibrose hepática está associado à remoção da sua causa, como a eliminação dos vírus das hepatites B e C ou abstinência alcoólica. Considerada anteriormente como sendo meramente o acúmulo de tecido cicatricial, atualmente é reconhecida como sendo um processo dinâmico que pode progredir ao longo do tempo. Porém, embora potencialmente reversível durante os estágios iniciais, um número significativo de pacientes evolui para fibrose avançada e cirrose terminal, aumentando o risco de carcinoma hepatocelular (HCC) (17). Muitas moléculas têm sido usadas com sucesso como agentes antifibróticos. Entre elas encontram-se inibidores do fator transformador de crescimento β (TGF- β) e o fator de crescimento hepático (HGF), uma citocina produzida pelas HSC e implicadas da regeneração celular (18). Entre os fármacos mais usados pode-se destacar a NAC (19), um fármaco conhecido principalmente por seu efeito antioxidante, sendo normalmente utilizado em pacientes em casos de intoxicação por paracetamol (20). Também foi demonstrado seu efeito preventivo *in vitro* sobre modelo experimental de cirrose, onde foram observados dois mecanismos de ação da NAC, diminuindo o estresse oxidativo e TGF- β (21). Por ser um potente antioxidante, a NAC é utilizada como controle positivo em estudos que avaliam a atividade antioxidante de substâncias (22). O ácido biliar ursodesoxicólico (Usordiol), também é utilizado como agente terapêutico e pode reduzir o dano hepatocelular e a fibrose, agindo indiretamente como antioxidante pela prevenção da peroxidação induzida pelos ácidos biliares (23). A silimarina é um composto natural com atividade hepatoprotetora e antioxidante, devido a sua capacidade de inibir os radicais livres que são produzidos a partir do metabolismo de substâncias tóxicas, como etanol e CCl₄. Estudos recentes demonstraram que este composto pode aumentar a síntese proteica e a regeneração hepatocelular, conservar a fluidez da membrana plasmática, suprimir a fibrinogênese e induzir a fibrólise hepática (24, 25).

Com relação ao carcinoma hepático, atualmente a ressecção cirúrgica tem sido considerada o tratamento chave, havendo, porém, recorrência do HCC em aproximadamente 80% dos pacientes dentro de um período de cinco anos,

principalmente pela carcinogênese multicêntrica latente ou metástase intra-hepática (26). Além disso, o uso deste tratamento no HCC multinodular é controverso. Neste caso, a literatura sugere que a melhor alternativa é o transplante. O transplante de fígado elimina não apenas o tumor, mas também a doença hepática subjacente com excelentes resultados, alcançando um índice de sobrevivência superior a 60% em cinco anos, porém, muitos pacientes não são candidatos ao transplante por causa do tamanho do tumor, idade avançada, custos elevados e, finalmente, escassez de órgãos (27).

A quimioterapia também é uma modalidade amplamente utilizada no tratamento de HCC, consistindo na utilização de agentes químicos, isolados ou em combinação com outros medicamentos, ou com outras terapias (cirurgia, radioterapia). Apesar de ser amplamente utilizada, apresenta altos índices de óbito precoce (primeiro mês) devido à toxicidade do tratamento, sendo a sepse em pacientes com neutropenia a causa mais comum (28).

1.4. CPBMF65 E O PAPEL DA URIDINA NAS DOENÇAS HEPÁTICAS E NO CÂNCER

No intuito de buscar tratamentos mais eficazes para fibrose hepática e/ou câncer, novos fármacos estão sendo desenvolvidos com alvos moleculares definidos, a fim de atingir rotas metabólicas. Um destes fármacos é o 5-ciano-4-metil-6-oxo-1,6-diidropiridin-2-olato de potássio (CPBMF65) (Figura 1), um inibidor da enzima uridina fosforilase 1 humana (UPP1) (29).

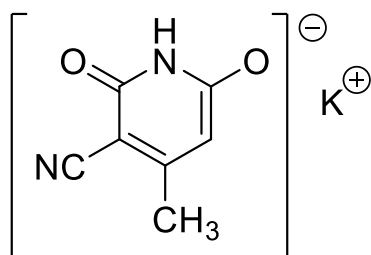


Figura 1 – Estrutura de CPBMF65 (C₇H₅KN₂O₂).

Fonte: Adaptada de Renck D et al. (29)

A UPP1 controla a concentração celular da uridina (Urd), através da fosforólise reversível de Urd à uracil e ribose-1-fosfato na presença de fosfato inorgânico (30), utilizando a via de salvamento de pirimidinas. A Urd é um nucleosídeo natural de pirimidina envolvido em processos celulares como síntese de RNA e um modulador bioquímico promissor para reduzir a toxicidade causada por quimioterápicos como o 5-fluorouracil (5-FU), sem prejudicar sua atividade anti-tumoral (31).

Estudos recentes mostraram a relação entre o metabolismo das pirimidinas e doenças hepáticas, sugerindo que a Urd pode ter um efeito protetor, justificado pela redução de sua concentração em doenças hepáticas crônicas (32). Também foi demonstrado que a Urd diminui a inflamação e a fibrose pulmonar induzida pela bleomicina, diminuindo a produção de colágeno (33). Além disso, os inibidores da UPP1 (que aumentam as concentrações celulares de Urd) também podem ter efeito sobre células tumorais, pois a enzima tem expressão aumentada em vários tumores sólidos humanos quando comparada aos tecidos normais. Isto acontece, possivelmente, devido às frequentes mutações de p53, supressor da UPP1, ou à expressão elevada de várias citocinas (indutoras da expressão de UPP1) (34). O uracil também é consumido muito mais rapidamente em células tumorais do que em normais, devido ao aumento da sua proliferação (35).

2. JUSTIFICATIVA

Em função da escassez de tratamentos e dos diversos efeitos adversos apresentados pelos que são utilizados atualmente, é evidente a importância da busca de novas substâncias que possam minimizar estes efeitos sem comprometimento da eficácia.

Com base na potencial relação do aumento de Urd com a possível progressão e/ou reversão de doenças hepáticas crônicas (fibrose e câncer), acreditamos que o inibidor da UPP1, CPBMF65, possa interromper parcialmente a via de salvamento das pirimidinas, provocando efeito antifibrótico *in vitro* e *in vivo* e diminuindo a proliferação de células de hepatocarcinoma *in vitro*.

3. OBJETIVOS

3.1. OBJETIVO GERAL

Este trabalho tem por objetivo avaliar a atividade antiproliferativa da molécula sintética (CPBMF65) em células de fibrose hepática GRX e de hepatocarcinoma HepG2 e a sua ação hepatoprotetora em camundongos C57BL/6 com fibrose induzida por tetracloreto de carbono (CCl₄), determinando os mecanismos envolvidos.

3.2. OBJETIVOS ESPECÍFICOS

3.2.1. AVALIAÇÃO DO EFEITO ANTIFIBRÓTICO HEPÁTICO *IN VITRO* E *IN VIVO*

- Determinar as concentrações de CPBMF65 que possuem efeito na inibição da proliferação celular da linhagem celular de GRX;
- Verificar a toxicidade da molécula através da liberação de LDH da célula para o meio de cultivo;
- Verificar se a droga provoca a reversão fenotípica através da avaliação de gotas de gordura no citosol celular;
- Verificar se a droga possui efeito sobre a senescência celular ou morte celular programada por apoptose;
- Avaliar o efeito sobre a contração celular do gel de colágeno;
- Avaliar a toxicidade e o efeito antifibrótico de CPBMF65 em camundongos C57BL/6 com fibrose induzida por CCl₄, através da avaliação de medidas das concentrações plasmáticas das transaminases aspartato amino transferase (AST) e alanina amino transferase (ALT), da fosfatase alcalina e das bilirrubinas;
- Avaliar a expressão gênica de colágeno tipo I e α -SMA no fígado dos camundongos;
- Avaliar o efeito do composto CPBMF65 sobre a histologia hepática.

3.2.2. AVALIAÇÃO DO EFEITO ANTINEOPLÁSICO HEPÁTICO *IN VITRO*

- Determinar as concentrações de CPBMF65 e uridina que possuem efeito na inibição da proliferação celular da linhagem celular de HepG2;
- Verificar a toxicidade de CPBMF65 e uridina através da liberação de LDH da célula para o meio de cultivo;
- Avaliar o efeito de excesso de uridina Urd como possível mecanismo de feedback negativo;
- Verificar se possuem efeito sobre o ciclo celular, senescência, autofagia ou morte celular programada por apoptose;
- Avaliar a influência sobre o estresse oxidativo celular.
- Avaliar a expressão gênica de p53 (ciclo celular e apoptose);
- Avaliar o tratamento crônico com CPBMF65 e Urd.

Os próximos capítulos estão organizados da seguinte forma:

- No capítulo 2 consta o artigo científico submetido para o periódico *European Journal of Pharmacology* e é composto pelos objetivos específicos **AVALIAÇÃO DO EFEITO ANTIFIBRÓTICO HEPÁTICO IN VITRO E IN VIVO.**
- No capítulo 3 consta o artigo científico submetido para o periódico *Toxicology in Vitro* e é composto pelos objetivos específicos **AVALIAÇÃO DO EFEITO ANTINEOPLÁSICO HEPÁTICO IN VITRO.**
- No capítulo 4 são apresentadas as considerações finais e as referências.

Capítulo 2

“Therapeutic effect of Uridine phosphorylase 1 (UPP1) inhibitor on liver fibrosis in vitro and in vivo”

Manuscrito enviado para o periódico European Journal of Pharmacology, 2019

**Therapeutic effect of Uridine phosphorylase 1 (UPP1) inhibitor on liver fibrosis in vitro
and in vivo**

Elisa Feller Gonçalves da Silva^{a,*}, Bruna Pasqualotto Costa^a, Marcella Tornquist Nassr^a,
Bruno de Souza Basso^a, Matheus Scherer Bastos^a, Camille Kirinus Reghelin^a, Maria Claudia
Garcia^a, Vitor Giancarlo Schneider Levorse^a, Leonardo Pfeiff Carlessi^a, Gabriela Viegas
Haute^a, Carolina Luft^a, Géssica Luana Antunes^a, Luiz Augusto Basso^b, Pablo Machado^b,
Jarbas Rodrigues de Oliveira^a

^a Laboratório de Pesquisa em Biofísica Celular e Inflamação, Pontifícia Universidade Católica do Rio Grande do Sul (PUCRS), Porto Alegre, Rio Grande do Sul, Brazil. Postal code: 90619-900

^b Centro de Pesquisas em Biologia Molecular e Funcional (CPBMF), Pontifícia Universidade Católica do Rio Grande do Sul (PUCRS), TecnoPuc, Porto Alegre, Rio Grande do Sul, Brazil. Postal code: 90619-900

*Corresponding author.

E-mail address: elisa.feller@acad.pucrs.br

Abstract

Potassium 5-cyano-4-methyl-6-oxo-1,6-dihydropyridine-2-olate (CPBMF65) is a potent inhibitor of the uridine phosphorylase 1 (UPP1) enzyme. Its non-ionized analog has already demonstrated biological properties by reducing adverse effects caused by the chemotherapeutic 5-fluorouracil (5-FU). In addition, it has been demonstrated that uridine inhibits inflammation and fibrosis in bleomycin lung injury, decreasing collagen production. The purpose of this study was to investigate the *in vitro* and *in vivo* effects of CPBMF65 on activated hepatic stellate cells (HSC) and on carbon tetrachloride-induced liver fibrosis in mice. After incubation with CPBMF65, decreased cell proliferation and phenotype reversion were observed *in vitro*. After, CPBMF65 promoted a protective effect against tetrachloride-induced liver fibrosis in mice demonstrated by its antifibrotics and anti-inflammatory actions. The results of the present study indicate that this UPP1 inhibitor may have potential as a novel therapeutic agent for the treatment of liver fibrosis.

Keywords: uridine phosphorylase 1; hepatic stellate cells; liver fibrosis; carbon tetrachloride; lipid droplets; senescence.

1. INTRODUCTION

Liver fibrosis is the pathologic result of inflammatory liver diseases, characterized by activated Hepatic stellate cells (HSC) proliferation, inability to store vitamin A in cytoplasmic lipid droplets, increased expression of α -smooth muscle actin (α -SMA) and profibrotic genes (Basso et al., 2019). This process is associated with chronic injury, including viral infection, alcohol abuse and steatosis that leads to accumulation of fibrotic matrix rich in collagen and at later stages can cause liver failure and mortality (Barcena et al., 2019). However, as has been previously described, liver fibrosis is potentially reversible (Shin et al., 2018).

Antifibrotic agents targeting HSC activation have been proposed as a therapeutic target against liver fibrosis. Uridine phosphorylase is a key enzyme in the pyrimidine salvage pathway, catalyzing the reversible phosphorolysis of uridine (Urd) to uracil and ribose-1-phosphate. The human uridine phosphorylase type 1 (UPP1) is a molecular target of inhibitors proposed to increase Urd levels to prevent adverse effects of chemotherapeutic agents like 5-fluorouracil (Renck et al., 2010). The therapeutic potential of Urd has also been assessed in disorders such as cystic fibrosis and liver dysfunction (Weinberg et al., 2011). Moreover, the study of Cicko et al. demonstrated that Urd have anti-inflammatory and anti-fibrotic effects in animal models of pulmonary fibrosis. In addition, Urd treatment also inhibited the synthesis of collagen, leading to a reduction in collagen deposition in the lung (Cicko et al., 2015).

Selective inhibitors of UPP1 have been proposed to increase Urd levels. Urd is one of the five standard molecules that comprise nucleic acids, involved in cellular processes such as RNA synthesis. Exogenous administration of Urd is not well tolerated, since higher doses would have to be administered in order to have some effect due to the rapid degradation caused by UPP1 (Pizzorno et al., 2002).

The potassium 5-cyano-4-methyl-6-oxo-1,6-dihydropyridine-2-olate (CPBMF65), an inhibitor of UPP1, is a new molecule, synthesized and produced at the Pontifícia Universidade Católica do Rio Grande do Sul (PUCRS), and tested in the study of Renck et al. (Renck et al., 2013) to verify the 5-fluorouracil toxicity decrease in SW-620 cells. The present study aimed to investigate the effects of the UPP1 inhibitor, CPBMF65, on hepatic stellate cells (GRX), and on carbon tetrachloride-induced liver fibrosis in mice, to further demonstrate the possible/potential therapeutic effect of CPBMF65 on liver fibrosis.

2. MATERIALS AND METHODS

2.1 HSC cell culture

GRX hepatic stellate cell line was obtained from the Rio de Janeiro Cell Bank (Federal University, Brazil). The medium used for cell culture was Dulbecco's Modified Eagle Medium (DMEM), supplemented with 5% fetal bovine serum (FBS) (Invitrogen, USA), 2 g/L HEPES buffer, 3.7 g/L NaHCO₃, and 1% penicillin and streptomycin (Invitrogen, USA) and pH 7.4. Cells were incubated with CPBMF65 for 120 hours at 37 °C under a humidified atmosphere containing 5% CO₂. All experiments were done three times.

2.2 In vitro treatment with CPBMF65

Plates were incubated at 37 °C in a humidified atmosphere with 5% CO₂ for 120 hours, aiming to perform a dose-response curve and also to determine the cytotoxicity of CPBMF65 (Fig.1). Different concentrations (7.5, 15, 45 and 90 µM) diluted in DMEM medium with 5% FBS were tested. N-acetylcysteine (NAC; 400 µM, Farmashop, Brazil), was used as a positive control. The control group consisted of GRX cell on culture medium for all experiments. The 120-hour treatment time was determined after a previous time-curve performed in our laboratory. All experiments were done three times.

2.3 Evaluation of cellular proliferation

The Trypan Blue exclusion assay was used to assess viability and cell growth/proliferation. Cells were seeded and treated as described above. After 120 hours of incubation, the number of viable cells was determined by mixing 25 µl of cell suspension and 25 µl of 0.4% Trypan Blue (Sigma-Aldrich, USA) using a Neubauer hemocytometer and optical microscope (Nikon Optiphot, Japan). Blue cells were counted as dead cells and those that did not absorb the dye, as living cells. The results were expressed as the absolute number of cells per culture well.

2.4 Measurement of lactate dehydrogenase

The cytotoxicity of the treatments was evaluated by the presence of the enzyme lactic dehydrogenase in the external environment, since the release of lactate dehydrogenase (LDH) (lactate dehydrogenase enzyme located in the cytoplasm) in the culture medium is considered

evidence of cell membrane rupture. Enzyme activity was measured in both (supernatants and lysates) using the colorimetric lactate dehydrogenase kit (Labtest, Brazil). As control of cell lysis, we used Tween 5% (Sigma-Aldrich, Germany) in the culture medium. LDH release was calculated by measuring the absorbance at 340 nm using an ELISA microplate reader. All experiments were performed in triplicate and repeated three times.

2.5 Detection of GRX cells lipid droplets

The estimation of cell accumulation of lipid droplets was observed using Oil Red (ORO; Sigma Chemical Co., USA) assay. After 120 hours of treatment with selected concentrations of CPMF65 (7.5 and 90 μM) and NAC 400 μM , cells were fixed with 10% formaldehyde for 1h and stained with ORO. Intracellular lipid accumulation was observed after 30 minutes, using an inverted light microscope at a magnification of 400x. The ORO was extracted using isopropanol and the absorbance was read at 340 nm using an ELISA microplate reader. Specific lipid content was calculated as the ratio of absorbance value obtained for ORO and number of counted cells.

2.6 Evaluation of apoptosis and senescence

The Nuclear Morphometric Analysis (NMA) is based on the evaluation of the size and shape of the nucleus of eukaryotic cells *in vitro*. This technique enables the assessment of the number of apoptotic or senescent cells. Cells were seeded in 24-well plates with a cell density of 5×10^4 per well. The selected doses of CPBMF65 (7.5 and 90 μM) were used. After 120 hours of treatment, the culture medium was discarded and four steps were performed: (1) labeling of the nuclei with DAPI (4', 6-diamidino-2-phenylindole), a fluorescent dye that binds strongly to the adenine-rich regions and thymine in DNA sequences (Kim et al., 2012); (2) acquisition of images by inverted fluorescence microscope (Eclipse TE2000-S, Nikon, Japan); (3) obtaining the morphometric data (Image Pro-Plus 4.5 software, Media Cybernetics, USA); (4) data analysis (Excel 2013), according to the protocol described by Filippi-Chiela et al. (Sperotto, 2014). As an apoptosis positive control, was used 2.5 μM . Cisplatin (CDDP) and as a senescence positive control, we used 150 μM hydrogen peroxide (H_2O_2) (Zdanov et al., 2006).

2.7 Assessment of GRX cells contraction by collagen gel analyses

Collagen from rat tail tendon was extracted and prepared as described by Rejan et al. (Rajan et al., 2006). Collagen gels (125 μ l of 4x DMEM and 125 μ l of 4 mg/ml rat tail tendon collagen) were impregnated with 1×10^5 cells resuspended in 250 μ l of PBS. Gels were added to a 24-well plate, left to polymerize for 30 minutes at 37 °C, detached and suspended in 600 μ l of DMEM with 5% FBS alone or with CPBMF65 and NAC. Images were obtained after 24 hours and the surface of the area of each gel was determined as the percentage of well area, using the software Image-Pro Plus 4.5 (Media Cybernetics, USA).

2.8 Mouse model of carbon tetrachloride induced liver fibrosis

Male C57Bl/6 mice (8-12 weeks old) were kept under standard conditions of temperature (22 ± 2 °C), light (12 hours light-dark cycle) and humidity (50-70%), in individually ventilated cages, receiving standard rodent chow and tap water ad libitum. They were obtained from the Central Animal House of the Pontifícia Universidade Católica do Rio Grande do Sul (CeMBE; PUCRS; Brazil). The experimental protocol was approved by the Ethics Research Committee of Pontifícia Universidade Católica do Rio Grande do Sul (CEUA-PUCRS, CEUA 7088) and maintained in accordance with the Guiding Principles in the Care and Use of Animals approved by the Council of the American Physiological Society. All the administrations were carried out at 1:00 PM to avoid a possible influence of circadian cycle variation on UPP1 activity.

2.9 Survival curve

The animals were randomly divided in two groups and treated during the period of 15 days. The animals of the first group received intraperitoneal 50 mg/Kg daily (i.p) injections of CPBMF65 dissolved in dimethyl sulfoxide (DMSO). Mice in the second group, were divided per dosage of CPBMF65 at 0, 6, 12, 25 and 50 mg/Kg, dissolved in DMSO, and received i.p. injections every other day (qod). The survival rate for two groups were constructed based on Kaplan Meier Survival Analysis using the software Graphpad Prism 5 (Graphpad Software Inc., USA). After 15 days of treatment, mice were sacrificed, and we proceeded with serological tests.

2.10 CCl₄ model of liver fibrosis and CPBMF65 administration

Mice received i.p. injections of CCl₄ at the dosage of 1 ml/Kg body weight (diluted in olive oil) three times a week (CCl₄ group) or vehicle (olive oil three times a week and DMSO twice a week) (Vehicle Control). For the treated group, animals received i.p. CCl₄ 1ml/Kg (diluted in olive oil) three times a week and CPBMF65 2 mg/Kg (dissolved in DMSO) twice a week (CCl₄+CPBMF65 group). After 10 weeks of treatment, all animals were euthanized, and serum and liver sections were collected.

2.11 Biochemical analyses

Serum aspartate aminotransferase (AST), alanine aminotransferase (ALT), total bilirubin, albumin, and alkaline phosphatase were determined with a commercial assay kit according to manufacturer's instructions (Labtest, Brazil).

2.12 RNA isolation and quantitative PCR

Samples of total RNA from mouse liver tissues were extracted by Trizol reagent (Invitrogen, Thermo Fisher, Inc., USA), according to manufacturer's instructions. cDNA was synthesized from 1µg RNA using Superscript III First-Strand Synthesis SuperMix (Invitrogen, Thermo Fisher, Inc., USA) according to the manufacturer's instructions. Primer sequences for mouse samples were as follows: α -smooth muscle actin (α -SMA), forward 5'-ACTGGGACGACATGGAAAAG-3', and reverse, 5'-ATCTCCAGAGTCCAGCACA-3'; collagen I forward, 5'-GAGCGGAGAGTACTGGATCG-3', and reverse, 5'-TACTCGAACGGGAATCCATC-3'; GAPDH, forward 5'-GTGGCAAAGTGGAGATT-3' and reverse, 5'-GTGGAGTCATACTGGAACA-3'. A final concentration of 1.4pmol/µL for each primer and SYBR Green I Master Mix (total volume of 10 µL) were used for the reaction mix. PCR amplifications were performed in a Step One™ real-time PCR system (Applied Biosystems, Thermo Fisher, Inc., USA) using the standard protocol. Data were analyzed with GAPDH as a reference gene (control). Results are expressed as fold expression relative to expression in the control group using the $\Delta\Delta C_t$ method.

2.13 Liver histopathology analysis

Liver samples were fixed in 10% buffered formalin, paraffin embedded, and the tissue was cut into 5 µm sections. H&E-stained liver sections were assessed by semi-quantitatively: steatosis (0-3), inflammation (0-2), and ballooning (0-2). To demonstrate fibrosis, liver

sections were stained with Picro Sirius Red. Liver fibrosis also was semi-quantitatively determined: fibrosis (0-4). Images were captured through BMX 43 microscope equipped with camera DP73 (Olympus, Japan).

2.14 Statistical analysis

Results were presented through descriptive statistics (mean and standard deviation). Survival rate was analyzed by Kaplan-Meier method (Goel et al., 2010). For the comparison of means between groups, we used the one-way analysis of variance (ANOVA) followed by the Tukey post-hoc test for multiple comparisons. The significance level was set at $p < 0.05$ with a 95% confidence interval and all data were analyzed using SPSS (Statistical Package for Social Sciences), version 15.0. (SPSS Inc., USA).

3. RESULTS

3.1 Effect of CPBMF65 on GRX cell proliferation and LDH liberation. Firstly, we have assessed the antiproliferative effect of CPBMF65 at doses of 7.5, 15, 45, 90 μM and NAC 400 μM (positive control) in GRX cells. Figure 1A shows decreased proliferation at all concentrations tested. The membrane integrity of GRX cells treated with CPBMF65 was also analyzed by measuring LDH in the cell supernatant and lysate. Cells were treated with the chosen concentrations of CPBMF65 (7.5 and 90 μM , the lowest and the highest concentration with significant result from our previous experiment) in order to determine its toxicity to cells. There were no significant differences between treatments and control, indicating no significant increase in cell death associated with necrosis in the treated groups as compared to the control group (Figure 1B). Experiments were performed in triplicate and repeated three times with similar results.

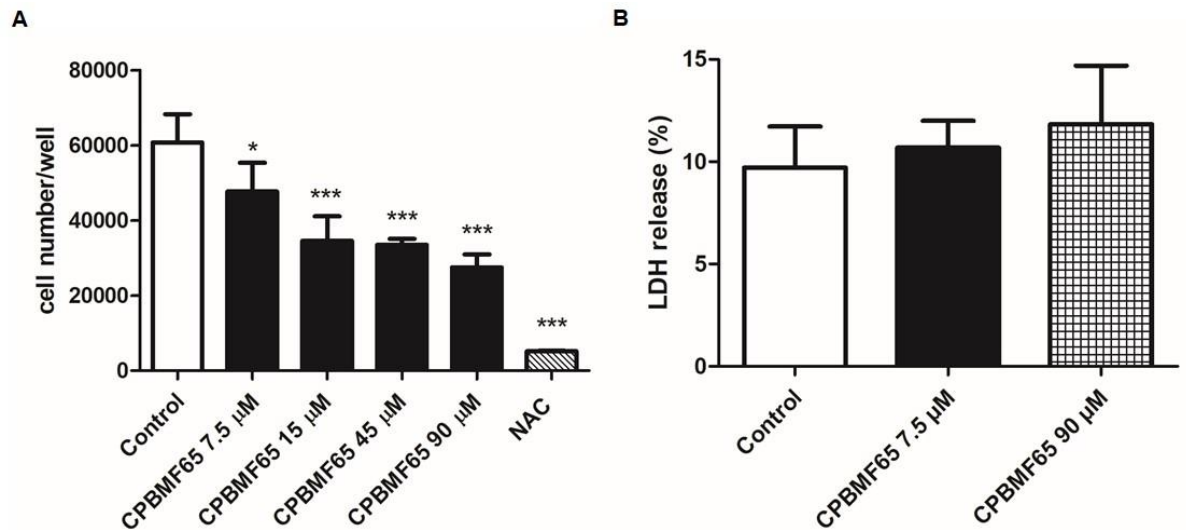


Figure 1: Effects of CPBMF65 on GRX cells proliferation and LDH release. **(A)** GRX cells were treated with CPBMF65 (7.5-90 μ M) and NAC 400 μ M for 120 h and cell number was assessed by direct cell count. Cellular proliferation was assessed by Trypan blue exclusion. Data represent the mean \pm SD. Results were expressed as cell number/well. (* P <0.05, *** P <0.0001 vs control, n =3); **(B)** Percent of LDH release of GRX cells after 120 hours of treatment with CPBMF65 7.5 and 90 μ M.

3.2 CPBMF65 induce phenotypic reversion on GRX cells. The ability of CPBMF65 to revert activated HSC by accumulation of lipids in cytoplasm was investigated. GRX cells treated with CPBMF65 concentrations showed to increase the ability of storing fat in cytoplasm. NAC treatment also shows a significant increase in fat droplets (Figure 2 A, B).

Lipid accumulation was quantified by absorbance at 492 nm and confirmed the result of the CPBMF65 on storing lipids by GRX cells (Figure 2 B).

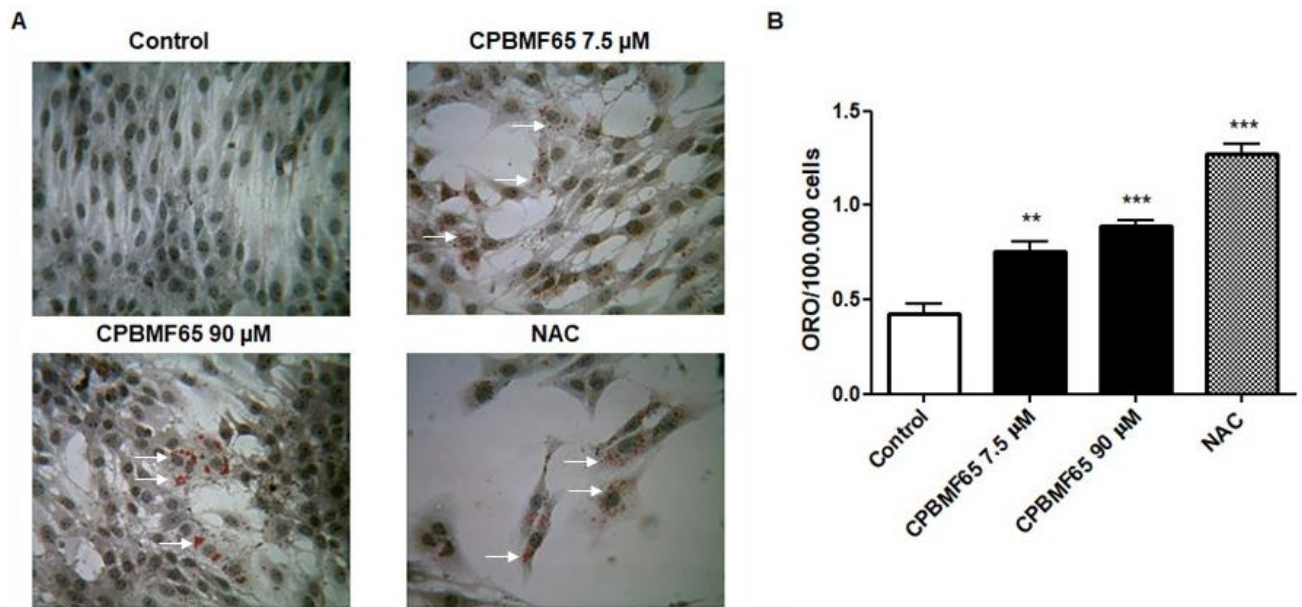


Figure 2: (A) Oil Red-O (ORO) staining of GRX cells at 120 hours for Control, CPBMF65 7.5 and 90 μM and NAC 400 μM , (B) Lipid quantification of GRX cells. Results are shown as the absorbance value obtained for ORO adjusted for number of 5×10^4 cells. Data presented as mean \pm SD (**, *** $P < 0.001$ vs control, $n=3$). Arrows indicate the lipid droplets.

3.3. Effect of CPBMF65 on GRX cells senescence. Another mechanism that may be involved in reversion of activated HSC is senescence (Krizhanovsky et al., 2008). We had chosen CPBMF65 7.5 and 90 μM , the lowest and the highest doses, respectively, with a significant antiproliferative effect to proceed with NMA experiments. The positive control, H_2O_2 150 μM , was chosen based on the work of Zdanov et al. (Zdanov et al., 2006). We have observed a 21% and 24% senescence increase in CPBMF65 cells treated with CPBMF65 7.5 and 90 μM , respectively, and 30% in those treated with H_2O_2 (positive control). We also investigate if the decreased in cell proliferation was due apoptosis, where the nuclei were stained with DAPI (NMA experiment). The positive control, CDDP 2.5 μM , was chosen based on previous studies of our laboratory. Quantification by NMA showed no significant difference between the CPBMF65-treated and control groups. The CDDP (positive control) had a 38% apoptosis increase (Figure 3).

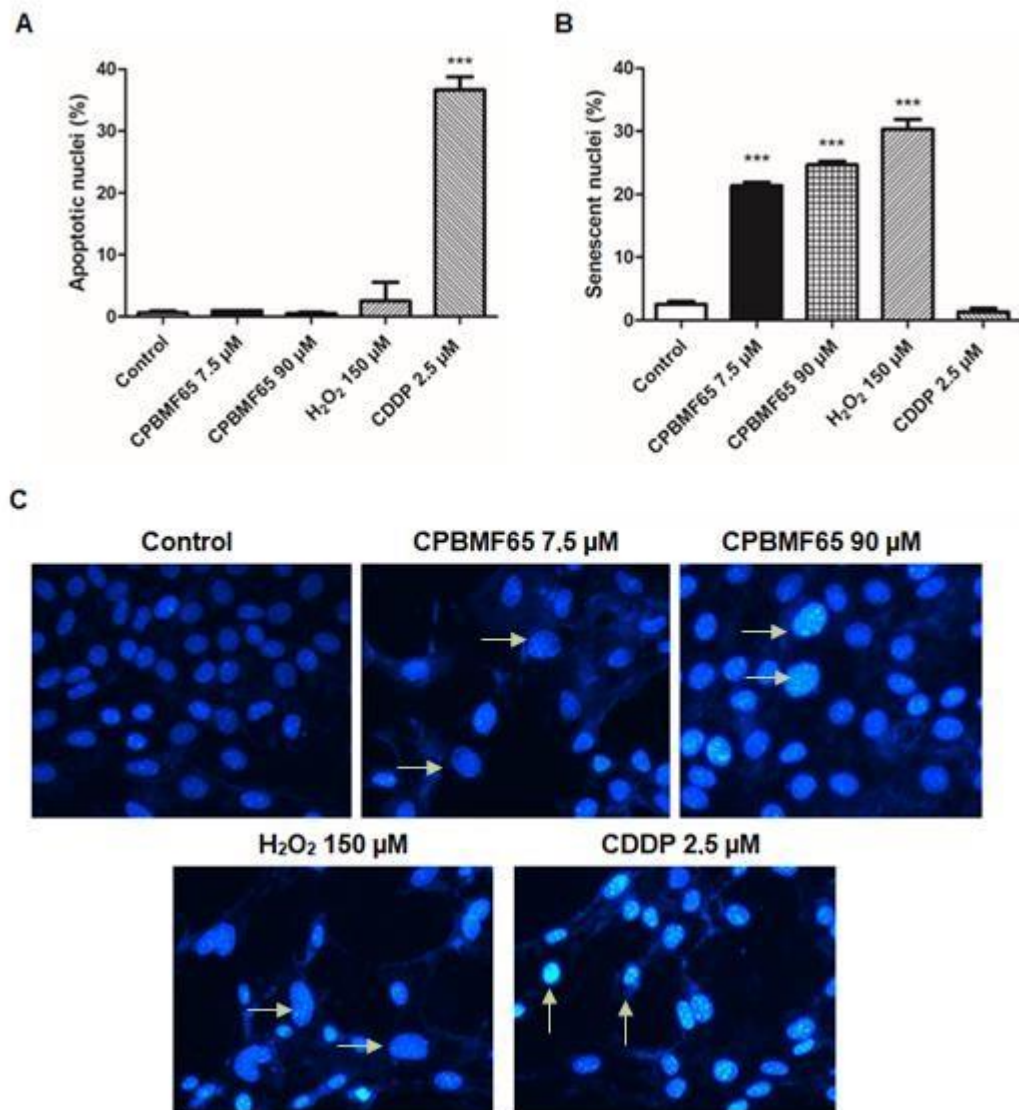


Figure 3: DAPI nuclei staining. Effect of CPBMF65 7.5, 90 µM, H₂O₂ 150 µM and CDDP on cell senescence and apoptosis of GRX cells analyzed by nuclear morphology. Cells were treated for 120 hours and data presented as mean ± SD (***P<0.001 vs control, n=3). CDDP was used as positive control of apoptotic inducer and H₂O₂ as a positive control of senescence inducer. The horizontal arrows indicate the senescent nuclei and the vertical arrows indicate the apoptotic nuclei.

3.4. Collagen gel assay. After 24 hours of treatment was possible to observe that the area occupied by collagen gel that received treatment with CPBMF65 or NAC was larger in relation to the area of the control group. Therefore, all treatments can decrease cell

contraction, whereas a greater contraction was detected in the control group, likely due to its activate phenotype (Figure 4).

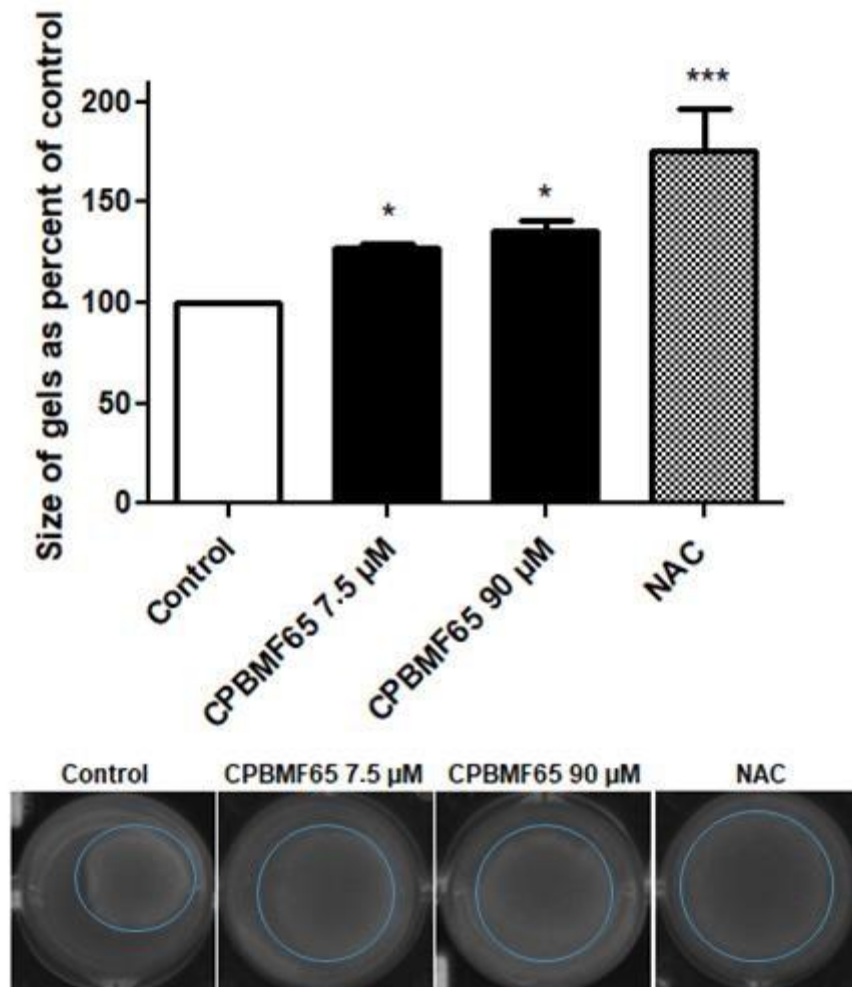


Figure 4: Cell contraction assessed by collagen gel assay in GRX cells. Cells were treated for 24 hours and data presented as mean \pm SD (* P <0.05, *** P <0.001 vs control, n =3).

3.5 Evaluation of CPBMF65 toxicity in vivo. Using Kaplan-Meier survival analysis, we could verify if CPBMF65 treatment would be safe for animals. The survival curve was designed using 2 treatment groups. The first group received 50 mg/kg i.p. injections daily. After 15 days, all the animals died. The second group received CPBMF65 6, 12, 25 or 50 mg/kg i.p. injections every other day (qod). All the animal survived, in the period of 15 days of treatment. Results showed that we could use i.p. injections every other day for the

inductions analyses (Figure 5). With the animals that survived, we proceeded with serological tests.

Survival of Two groups: Survival proportions

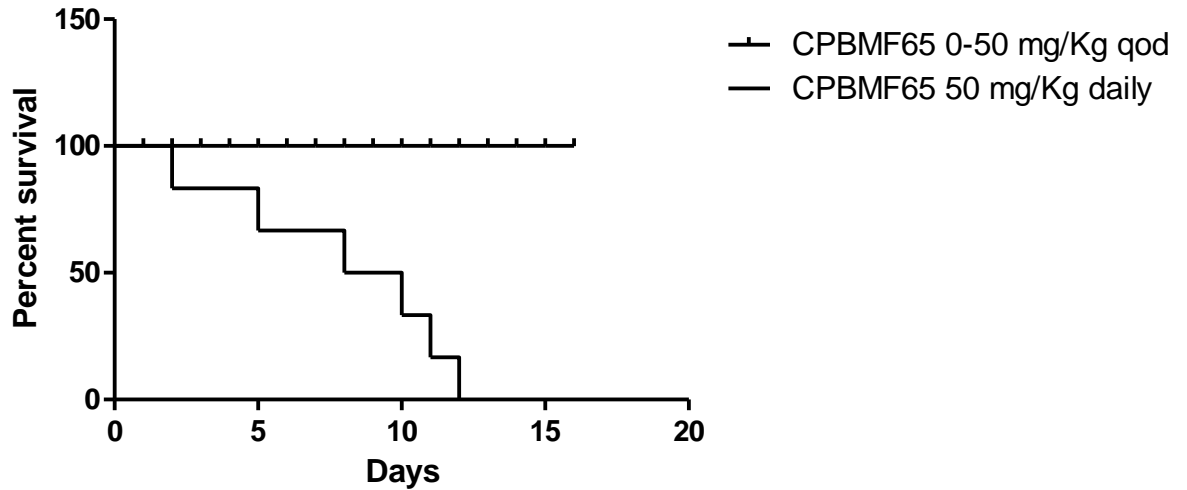


Figure 5: Kaplan-Meier survival analyses survival curve during the treatment period. The curve is different between the daily and the qod groups ($***P < 0.001$). P-value was calculated by log-Rank test.

3.6 Serum analyses for survival group of CPBMF65 i.p. injections. In order to verify if the treatment with CPBMF65 is not toxic to the animals, we proceed with serological tests of ALT, AST and Total Bilirubin. The results showed that the treatment of CPBMF65 i.p. injections of 6-50 mg/kg qod, does not appear to be toxic for the liver or interfere with hepatic functions (Figure 6).

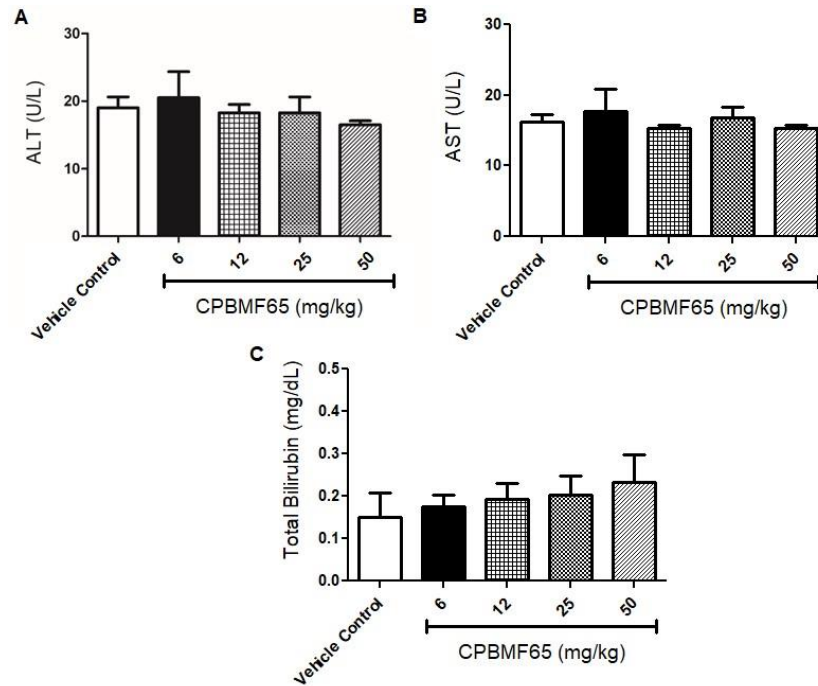


Figure 6: Serum analyses of CPBMF65 qod i.p. injections. Hepatic parameters: ALT, AST and Total Bilirubin. For all parameters, comparison between Vehicle Control and 6-50 mg/kg of CPMF65. Data presented as mean \pm SD.

3.7 CCl₄ model of liver fibrosis, CPBMF65 administration and Serum analyses. Based on the previous test we chose to use CPBMF65 2mg/kg i.p. injections, because induction has a longer treatment period. After 10 weeks treatment, all animals were killed. Animal serum were collected and tested for hepatic parameters (Alkaline phosphatase, Albumin, AST and ALT). For treated group (CCl₄+CPBMF65), ALT had a significant decrease in relation to the induction group (CCl₄), showing a possible protective effect of CPBMF65. For the other parameters, there was no significant difference between groups (Figure 7).

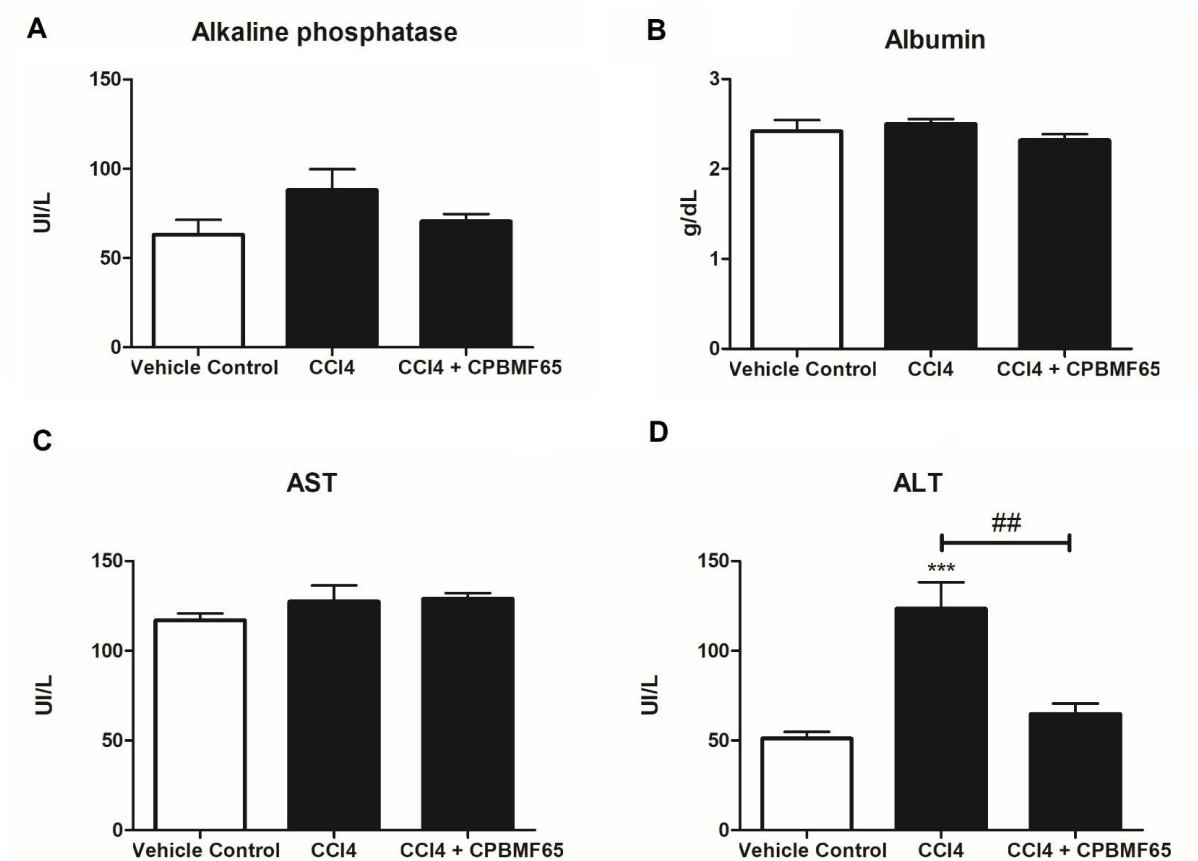


Figure 7: Serum analyses of induction groups. Hepatic parameters: alkaline phosphatase, albumin, AST and ALT. Data presented as mean \pm SD (***P<0.001 vs control, ##P<0.05 CCl₄ vs CCl₄+CPBMF65).

3.8 Expression of Collagen I and α -SMA. The relative expression of fibrogenic genes, Collagen I and α -SMA, relates to liver fibrosis. In order to elucidate if the CPBMF65 could decreased the expression of those genes, the differential expression of Collagen I and α -SMA was assessed. The results show that the relative expression of Collagen I or α -SMA are decreased in the treated group (CCl₄+CPBMF65) when compared to the induction group (CCl₄) (Figure 8).

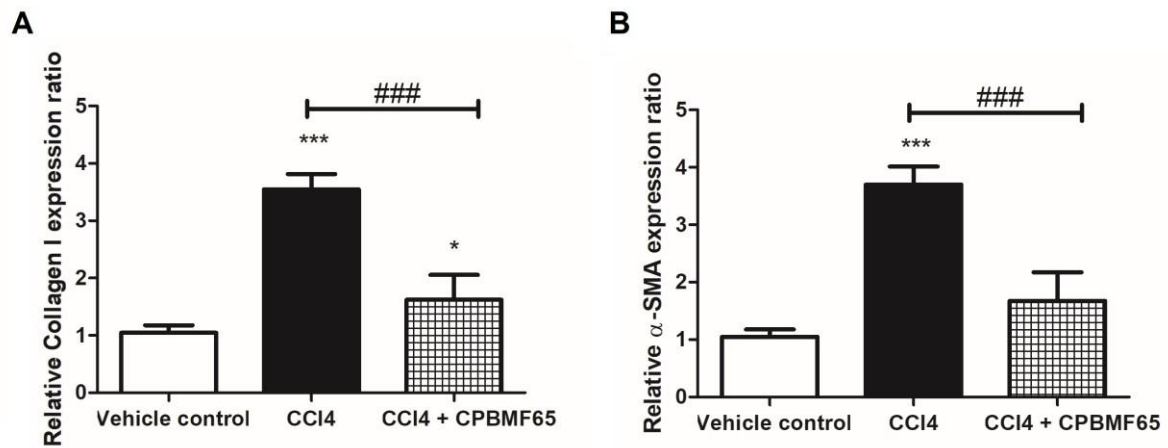


Figure 8: Effect of CCl₄ induction and treatment with CPBMF65 on relative Collagen I and α -SMA expression in mouse liver tissue. Data presented as mean \pm SD (*P<0.05 and ***P<0.001 vs control, ###P<0.001 CCl₄ vs CCl₄+CPBMF65).

3.9 CPBMF65 attenuates liver injury and fibrosis by CCl₄. We examined the putative role of CPBMF65 in preventing fibrosis *in vivo* (Figure 9) using an established mouse model in which hepatic damage is produced by repetitive cytotoxic CCl₄ injections. Results show that treatment with CPBMF65 reduce the fibrotic area, inflammation, steatosis and ballooning scores when compared to induced group (CCl₄).

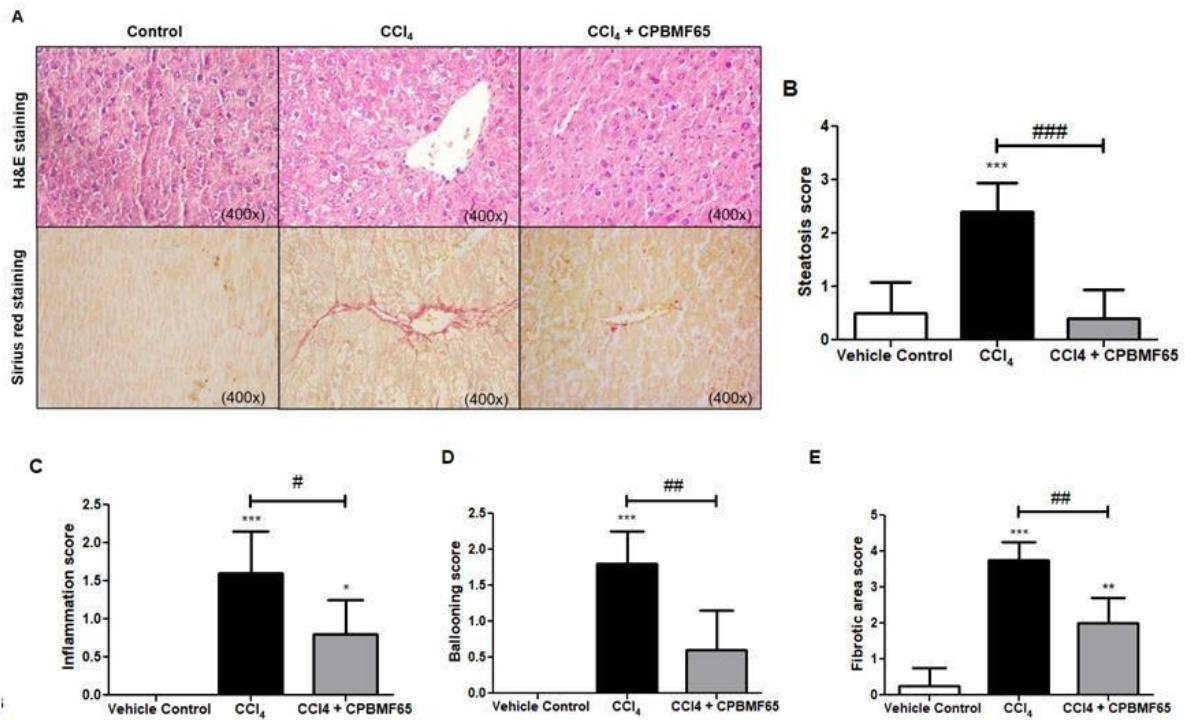


Figure 9: CPBMF65 administration reduces CCl₄-induced liver fibrosis in mice. (A) CCl₄ (fibrotic) but not vehicle control livers exhibit fibrotic scars. In CCl₄+CPBMF65 the fibrotic scar is visually reduced in comparison to CCl₄ group (evaluated by H&E and Sirius Red staining). (B) Steatosis score, (C) Inflammation score, (D) Ballooning score and (E) Fibrotic area score are reduced in CCl₄+CPBMF65 when compared to CCl₄. Data presented as mean ± SD (*, **P<0.05 and ***P<0.001 vs control, #, ###P<0.05 and ####P<0.001 CCl₄ vs CCl₄+CPBMF65).

4. DISCUSSION

Fibrosis is defined as the overgrown, hardening or scarring of tissues that could be transformed in a catastrophic tissue damage, contributing to a variety of pathologies, such as cirrhosis. There is no standard treatment for liver fibrosis, but several studies have revealed targets to prevent fibrosis progression (Bataller and Brenner, 2005). Traditionally, liver fibrosis is treated as an irreversible process, although recent studies point out new therapies that can result in significant regression of liver fibrosis (Povero et al., 2010). Treatment with CPBMF65, a new molecule that was used for the first time isolated and tested to explore its antiproliferative effects in GRX cells, reduced the proliferation at doses 7.5 to 90 μM in GRX

cells when compared to control. NAC is also tested as a positive control to prove the test efficacy.

Reduction of proliferation in GRX cells may be caused by necrosis (cytotoxicity) or for a programmed death mechanism. Therefore, aiming to demonstrate that this effect was not due to necrosis cytotoxicity, we have measured LDH, which did not demonstrate correlation between the ceasing of cell proliferation and death due to necrosis in GRX cells. We have also used trypan blue, which demonstrated absence of necrosis as well. HSCs serve as the main body storage compartment for vitamin A through lipid droplets. In the presence of liver injury, HSCs acquire an activate phenotype, characterized by an elevated expression of extracellular matrix, production of collagen I and α -SMA fibers, associated to lipid droplets loss (BobowskiGerard et al., 2018). Our results show a significant increase of lipid droplets evidenced by ORO staining, followed by a significant increase of senescence, demonstrated by the NMA analyses and reduction of contraction assessed by collagen gel assay in GRX cells treated groups.

Senescence of activated HSCs limits the fibrotic response to tissue damage by cell cycle arrest, reduced secretions of extracellular matrix components, enhanced secretion of extracellular matrix degrading enzymes, and enhanced immune surveillance (Krizhanovsky et al., 2008). Lipid droplets are abundant and enlarged in senescent cells, and treated cells with specific lipids induced senescence (Flor et al., 2017). The deactivation of HSCs is an important target, decreasing production of components of cellular matrix, resulting in reduction of contraction (Basso et al., 2019). Therefore, we can correlate the increased of lipid droplets and cell contraction decreased with senescence and probably with reduction of GRX cell proliferation.

Cicko et al. had demonstrated that Urd inhibits inflammation and fibrosis in bleomycin lung injury, decreasing collagen production (Cicko et al., 2015). CPBMF65 is an inhibitor of uridine phosphorylase, which creates the possibility of increased intracellular Urd during treatment. This means that when we increase intracellular Urd, it is possible to reduce cell proliferation, because this increase reflects the partial halt of the salvage pathway. The salvage pathway operates to recover bases and nucleosides generated from the breakdown of DNA and RNA. The salvaged bases can be then transformed into nucleotides and reincorporated into DNA. Nucleotides and nucleosides are regenerated and that can contribute to DNA formation, thus reactivating cell proliferation and growth (Squadrito et al., 2017).

Previous studies showed relation between pyrimidine metabolism and liver diseases and suggests that Urd could have a protective effect that could be explained by reduction in concentration in chronically disease livers (Schofield et al., 2017).

This study tested, for the first time, the effect of CPBMF65 in liver fibrosis. The i.p. treatment with CPBMF65 in male C57BL/6 animals on alternate days proved to be safe for the animals, a fact evidenced by the survival curve and the serological testes for liver parameters. In order to prevent liver damages caused by CCl₄-induced liver fibrosis in mice, we used CPBMF65 2mg/kg i.p. injections over the period of induction treatment. Levels of ALT are elevated, as well as α -SMA and collagen I expression ratio, by increased hepatic injury caused by CCl₄ treatment. In contrast, CPBMF65 treatment demonstrated the decreased of these levels, suggesting a protective effect of the molecule. Histological examination of liver sections from CCl₄ with CPBMF65 animals treated for 10 weeks, showed a statistically significant decreased in vesicular steatosis, inflammation, hepatocellular ballooning and fibrosis, hence approving its hepatoprotective effect.

Considering this work results, we believe that treatment with CPBMF65 can revert activated HSCs phenotype through increased of lipid droplets, reduction of contraction and can reduce GRX cells proliferation, probably supported by an increased senescent mechanism.

CPBMF65 promoted downregulation of HCS activation and seems to attenuate the liver fibrosis injury and inflammation in animal model of severe toxicity induced by CCl₄. Under these settings, CPBMF65 has a clear hepatoprotective effect, and should be considered as a potential agent to treatment liver fibrosis.

Conflict of interest statement

The authors declare no conflict of interest.

REFERENCE LIST

- Barcena, C., Aran, G., Perea, L., Sanjurjo, L., Tellez, E., Oncins, A., Masnou, H., Serra, I., Garcia-Gallo, M., Kremer, L., Sala, M., Armengol, C., Sancho-Bru, P., Sarrias, M.R., 2019. CD5L is a pleiotropic player in liver fibrosis controlling damage, fibrosis and immune cell content. *EBioMedicine*.
- Basso, B.S., de Mesquita, F.C., Dias, H.B., Krause, G.C., Scherer, M., Santarem, E.R., de Oliveira, J.R., 2019. Therapeutic effect of *Baccharis anomala* DC. extracts on activated hepatic stellate cells. *EXCLI journal* 18, 91-105.
- Bataller, R., Brenner, D.A., 2005. Liver fibrosis. *The Journal of clinical investigation* 115, 209-218.
- Bobowski-Gerard, M., Zummo, F.P., Staels, B., Lefebvre, P., Eeckhoutte, J., 2018. Retinoids Issued from Hepatic Stellate Cell Lipid Droplet Loss as Potential Signaling Molecules Orchestrating a Multicellular Liver Injury Response. *Cells* 7.
- Cicko, S., Grimm, M., Ayata, K., Beckert, J., Meyer, A., Hossfeld, M., Zissel, G., Idzko, M., Muller, T., 2015. Uridine supplementation exerts anti-inflammatory and anti-fibrotic effects in an animal model of pulmonary fibrosis. *Respiratory research* 16, 105.
- Flor, A.C., Wolfgeher, D., Wu, D., Kron, S.J., 2017. A signature of enhanced lipid metabolism, lipid peroxidation and aldehyde stress in therapy-induced senescence. *Cell death discovery* 3, 17075.
- Goel, M.K., Khanna, P., Kishore, J., 2010. Understanding survival analysis: Kaplan-Meier estimate. *International journal of Ayurveda research* 1, 274-278.
- Kim, T.M., Shin, S.K., Kim, T.W., Youm, S.Y., Kim, D.J., Ahn, B., 2012. Elm tree bark extract inhibits HepG2 hepatic cancer cell growth via pro-apoptotic activity. *Journal of veterinary science* 13, 7-13.
- Krizhanovsky, V., Yon, M., Dickins, R.A., Hearn, S., Simon, J., Miething, C., Yee, H., Zender, L., Lowe, S.W., 2008. Senescence of activated stellate cells limits liver fibrosis. *Cell* 134, 657-667.
- Pizzorno, G., Cao, D., Leffert, J.J., Russell, R.L., Zhang, D., Handschumacher, R.E., 2002. Homeostatic control of uridine and the role of uridine phosphorylase: a biological and clinical update. *Biochimica et biophysica acta* 1587, 133-144.
- Povero, D., Busletta, C., Novo, E., di Bonzo, L.V., Cannito, S., Paternostro, C., Parola, M., 2010. Liver fibrosis: a dynamic and potentially reversible process. *Histology and histopathology* 25, 1075-1091.
- Rajan, N., Habermehl, J., Cote, M.F., Doillon, C.J., Mantovani, D., 2006. Preparation of ready-to-use, storable and reconstituted type I collagen from rat tail tendon for tissue engineering applications. *Nature protocols* 1, 2753-2758.
- Renck, D., Ducati, R.G., Palma, M.S., Santos, D.S., Basso, L.A., 2010. The kinetic mechanism of human uridine phosphorylase 1: Towards the development of enzyme inhibitors for cancer chemotherapy. *Archives of biochemistry and biophysics* 497, 35-42.
- Renck, D., Machado, P., Souto, A.A., Rosado, L.A., Erig, T., Campos, M.M., Farias, C.B., Roesler, R., Timmers, L.F., de Souza, O.N., Santos, D.S., Basso, L.A., 2013. Design of novel potent inhibitors of human uridine phosphorylase-1: synthesis, inhibition studies, thermodynamics, and in vitro influence on 5-fluorouracil cytotoxicity. *Journal of medicinal chemistry* 56, 8892-8902.
- Schofield, Z., Reed, M.A., Newsome, P.N., Adams, D.H., Gunther, U.L., Lalor, P.F., 2017. Changes in human hepatic metabolism in steatosis and cirrhosis. *World journal of gastroenterology : WJG* 23, 2685-2695.
- Shin, G.M., Koppula, S., Chae, Y.J., Kim, H.S., Lee, J.D., Kim, M.K., Song, M., 2018. Anti-hepatofibrosis effect of *Allium senescens* in activated hepatic stellate cells and thioacetamide-induced fibrosis rat model. *Pharmaceutical biology* 56, 632-642.
- SPEROTTO, R.A.O., 2014. *Protocolos e métodos de análise em laboratórios de biotecnologia agroalimentar e de saúde humana*, 1 ed.
- Squadrito, F., Bitto, A., Irrera, N., Pizzino, G., Pallio, G., Minutoli, L., Altavilla, D., 2017. Pharmacological Activity and Clinical Use of PDRN. *Frontiers in pharmacology* 8, 224.

- Weinberg, M.E., Roman, M.C., Jacob, P., Wen, M., Cheung, P., Walker, U.A., Mulligan, K., Schambelan, M., 2011. Enhanced uridine bioavailability following administration of a triacetyluridinerich nutritional supplement. PloS one 6, e14709.
- Zdanov, S., Remacle, J., Toussaint, O., 2006. Establishment of H₂O₂-induced premature senescence in human fibroblasts concomitant with increased cellular production of H₂O₂. Annals of the New York Academy of Sciences 1067, 210-216.

Capítulo 3

“Uridine phosphorylase 1 (UPP1) inhibitor reduces HepG2 cell proliferation through cell cycle arrest and senescence”

Manuscrito enviado para o periódico Toxicology in Vitro, 2019

Uridine phosphorylase 1 (UPP1) inhibitor reduces HepG2 cell proliferation through cell cycle arrest and senescence

Elisa Feller Gonçalves da Silva^{a,*}, Kelly Goulart Lima^a, Gabriele Catyana Krause^a, Gabriela Viegas Haute^a, Leonardo Pedrazza^a, Anderson Velasque Catarina^b, Rodrigo Benedetti Gassen^c, Bruno de Souza Basso^a, Henrique Bregolin Dias^a, Carolina Luft^c, Maria Claudia Rosa Garcia^a, Luiz Augusto Basso^d, Márcio Vinícius Fagundes Donadio^a, Pablo Machado^d, Jarbas Rodrigues de Oliveira^a

^a Laboratório de Pesquisa em Biofísica Celular e Inflamação, Pontifícia Universidade Católica do Rio Grande do Sul (PUCRS), Porto Alegre, Rio Grande do Sul, Brazil. Postal code: 90619-900

^b Departamento de Ciências Básicas da Saúde, Universidade Federal de Ciências da Saúde de Porto Alegre (UFCSPA). Porto Alegre, Rio Grande do Sul, Brazil. Postal code: 90050-170

^c Laboratório de Imunologia Celular (IPB), Pontifícia Universidade Católica do Rio Grande do Sul (PUCRS), Porto Alegre, Rio Grande do Sul, Brazil. Postal code: 90619-900

^d Centro de Pesquisas em Biologia Molecular e Funcional (CPBMF), Pontifícia Universidade Católica do Rio Grande do Sul (PUCRS), TecnoPuc, Porto Alegre, Rio Grande do Sul, Brazil. Postal code: 90619-900

*Corresponding author.

E-mail address: elisa.feller@acad.pucrs.br

Abstract

Carcinoma Hepatocellular is the most prevalent type of tumor among primary tumors that reach the liver and the second cause of cancer-related death worldwide. The new synthetic compound named potassium 5-cyano-4-methyl-6-oxo-1,6-dihydropyridine-2-olate (CPBMF65) is a potent inhibitor of the uridine phosphorylase 1 (UPP1) enzyme. Its non-ionized analogue has already demonstrated biological properties by reducing adverse effects caused by the chemotherapeutic 5-fluorouracil (5-FU). Since UPP1 expression is increased in tumors compared to normal tissues, as well as its increase is directly linked to decreased p53 expression, we believe that CPBMF65 compound may have effects on the proliferation of neoplastic cell line HepG2. Cell proliferation, cytotoxicity, cell-cycle arrest, apoptosis, senescence, autophagy, reactive oxygen species, intracellular uridine, p53 expression and drug resistance were accessed. It was demonstrated after incubation that CPBMF65 decreases HepG2 cell proliferation through cell cycle arrest and senescence, increasing intracellular uridine and maintaining cell proliferation reduced during chronic treatment with the molecule. The results of present study indicate that UPP1 inhibitor reduces HepG2 cell proliferation through cell cycle arrest and senescence.

Key Words: uridine phosphorylase 1, HepG2 cells, hepatocellular carcinoma, cell-cycle arrest, senescence

1. INTRODUCTION

Hepatocellular carcinoma (HCC) is the sixth most common cancer and the second cause of cancer-related death in the world, with its incidence triplicated in the United States in the last three decades (Khan et al., 2015). It is a silent disease, usually detected at an advanced stage, which reduces the survival rate to approximately 14% within a five-year period (Sachdeva et al., 2015).

More than 50% of the cancers present mutation in the p53 protein (James et al., 2014). p53 acts like a sensor of nucleotide and nucleoside depletion. Then, in response to this depletion, DNA synthesis is arrested, activating p53, which suppress uridine phosphorylase 1 (UPP1) enzyme expression, once this enzyme catalyse the phosphorolysis of nucleoside uridine to uracil (Renck et al., 2014). The uridine accumulation results in partial halt of salvage pathway and p53 activation. Thus, a negative feedback regulation is established (Yan et al., 2006).

Uridine in combination with 5-benzylacyclouridine (BAU), a classic inhibitor of UPP1, has also show to protect mice against the neurotoxic side effects of 5-fluorouracil (5-FU) drug regimens, without affecting its antitumor activity (Zhang et al., 2001). UPP1 inhibitors may also have an effect on tumor cells, as the enzyme has increased expression in several human solid tumors when compared to normal tissues (James et al., 2014).

Selective inhibitors of UPP1 have been proposed to increase uridine (Urd) levels. Urd is a natural pyrimidine nucleoside involved in cellular processes such as RNA synthesis. Exogenous administration of Urd is not well tolerated, as very high doses would have to be administered in order to have some effect due to the rapid degradation caused by UPP1 (Pizzorno et al., 2002).

In the present study we used the potassium 5-cyano-4-methyl-6-oxo-1,6dihydropyridine-2-olate (CPBMF65), an inhibitor of UPP1. This new molecule, synthesized and produced at the Pontifical Catholic University of Rio Grande do Sul (PUCRS), was tested in the previous study of Renck et al. (Renck et al., 2013) to verify the 5-FU toxicity decrease in SW-620 cells.

Our work has the intention to propose the UPP1 inhibitor, CPBMF65, as a potential agent for the treatment of cancer, believing that this new molecule may interferes in the salvage pathway, inducing a cell proliferation decrease in the human hepatocarcinoma cell line, HepG2, by increasing p53 expression, through negative feedback.

2. MATERIALS E METHODS

2.1 HepG2 cell culture. HepG2 cells are from the American Type Culture Collection (ATCC). The medium used for cell culture was Dulbecco's Modified Eagle Medium (DMEM), supplemented with fetal bovine serum (FBS, 10%) under a humidified atmosphere containing 5% CO₂. Cells were initially seeded in 10 cm diameter plates and were used for the experiments when they had approximately 70% confluency and more than 95% viability in the trypan blue exclusion test. Seeding was performed one day prior to addition of the treatments, to allow cell adhesion.

2.2 Peripheral blood mononuclear cell preparation. The peripheral blood mononuclear cells (PBMC) were isolated from the blood of healthy human by gradient centrifugation on Ficoll-Paque (GE althcare). A total of 12 ml of heparinized blood was diluted 1: 2 with saline solution. Each 2 ml of Ficoll-Paque were added to 6 ml of the previous dilution and centrifuged at 720 x g at 22 °C for 20 minutes. After centrifugation, the supernatant was removed and ammonium chloride was added to lyse erythrocytes. The gradient was centrifuged at 200 x g at 4 °C for 10 minutes, this procedure was repeated twice. Afterwards, the cell pellet was washed twice in 10 ml of phosphate buffered saline (PBS). Cells were then re-suspended in RPMI 1640 medium supplemented with 0.15% garamycin (Schering-Plough) and 20% homologous serum at a final cell density of 2.0x10⁶ cells/ml. PBMC were used to verify whether treatment with CPBMF65 had effect on the viability and if there was toxicity to normal cells after 96 hours. Cell viability was observed, after 96 hours of treatment, by counting cells in a Neubauer chamber by Trypan Blue dye exclusion. This preparation had ≥ 95% of PMNs with a viability greater or equal to 90%. All reagents used were filtered through a disposable sterile filter unit 0.22 μM (Millex). All human subjects read and signed an informed consent form.

2.3 Treatment with CPBMF65 and Uridine (Urd). Plates were incubated at 37°C in a humidified oven with 5% CO₂ for 48 hours, aiming to perform a dose response curve and also to determine the cytotoxicity of CPBMF65 (new synthetic molecule called potassium 5cyano-4-methyl-6-oxo-1,6-dihydropyridine-2-olate, developed in PUCRS University) (Fig.1) in different concentrations (7.5, 15, 45, 90, 135 and 180 μM) and Urd (Sigma-Aldrich®) at concentrations of 1, 5 and 10 mM diluted in DMEM medium with FBS, 10%. The 48-hour treatment time was determined after a previous time-curve was performed in our laboratory and the concentrations chosen based on a previous study performed on SW-620 cells (Renck et al., 2013). All experiments were done three times.

2.4 Evaluation of cellular proliferation. The trypan blue exclusion assay was used to assess viability and cell growth/proliferation. Cells were seeded and treated as described above. After 48 hours of incubation, the number of viable cells was determined by mixing 25 μ l of cell suspension and 25 μ l of 0.4% tripan blue (Sigma-Aldrich, USA) using a neubauer hemocytometer and optical microscope (Nikon Optiphot, Japan). Blue cells were counted as dead cells and those that did not absorb the dye, as living cells. The result was expressed as absolute number of cells per culture well.

2.5 Measurement of lactate dehydrogenase. The cytotoxicity of the treatments was evaluated by the presence of the enzyme lactic dehydrogenase in the external environment, since the release of LDH (lactate dehydrogenase enzyme located in the cytoplasm) in the culture medium is considered evidence of cell membrane rupture. Enzyme activity was measured in both (supernatants and lysates) using the colorimetric lactate dehydrogenase kit (Labtest, Minas Gerais, Brazil). As a control of cell lysis, we have used Tween 5% in the culture medium. LDH release was calculated by measuring the absorbance at 492 nm using an Elisa microplate reader. All experiments were performed in triplicate and repeated three times.

2.6 Evaluation of autophagy. The evaluation of autophagy was performed using the acridine orange dye (AO). This acidotropic fluorogenic dye stains the cytoplasm and cell nuclei with green fluorescence and, when in an acid environment, undergoes physicochemical modifications and starts to emit red fluorescence (Chiela), indicating that the cells are in an autophagic process. The quantification of the degree of autophagy of the cells was performed on a flow cytometer. After 48 hours of treatment, cells were detached from the culture dish with trypsin and incubated with AO (1 μ g/ml) in culture medium for 15 minutes at room temperature and protected from light. Cells were then visualized by fluorescence microscope (Olympus IX71) and analyzed on FACSCanto II flow cytometer (BD Bioscience), evaluating the percentage of red fluorescence emitted using FlowJo 10.0.8 software (Tree Star Inc., Ashland, OR). As a positive control, cisplatin (CDDP) 20 μ M was used.

2.7 Evaluation of apoptosis. The PE-Annexin V/7AAD dual label assay was performed to quantify cells in apoptosis using the FACScan flow cytometer (Becton-Dickinson, USA). HepG2 cells were seeded in 96-well culture plates at a cell density of 2.5×10^4 cells per well. Selected doses of the drugs and 40 μ M of CDDP (positive control) were used. After 48 hours of the treatments, cells were trypsinized, washed with ice-cold PBS and resuspended in binding buffer at a cell density of 1×10^6 cells/ml. 5 μ l PE-Annexin V and 5 μ l 7-AAD were added, cells were homogenized and incubated for 15 minutes at room

temperature protected from light. After incubation, samples were analyzed by flow cytometry. Data was analyzed in the FlowJo 7.2.5 software program (Tree Star Inc., Ashland OR). The analysis allowed the discrimination between necrotic cells (Annexin V- / 7-AAD+), late apoptosis (Annexin V+ / 7-AAD+) and early apoptosis (Annexin V+ / 7-AAD).

2.8 Quantification of reactive oxygen species. We have also used the method of quantification of reactive oxygen species based on the application of 2', 7'-dichlorofluorescein diacetate (DCFH-DA) to evaluate the production of intracellular reactive oxygen species. DCFH-DA is a non-fluorescent substance that is converted to DCF (highly fluorescent) when oxidized by reactive oxygen and nitrogen species. HepG2 cells will be seeded in 96-well culture plates at a cell density of 2.5×10^4 cells per well. The selected doses were used and, after 48 hours of treatment, cells were removed from the culture dish using trypsin, washed with PBS and incubated with $10 \mu\text{M}$ DCFH-DA for 30 minutes at 37°C protected from light. The fluorescence intensity was evaluated on a fluorometer with an excitation wavelength of 485 nm and emission at 520 nm. As a positive control, we have used hydrogen peroxide (H_2O_2) at a concentration of $1000 \mu\text{M}$.

2.9 Evaluation of senescence. The NMA method is based on the measurement of size and shape of the nucleus of eukaryotic cells in vitro. This technique enables the evaluation of the number of senescence cells. Cells were seeded in 24-well plates with cell density of 5×10^4 per well. The selected doses of CPBMF65 and Urd were used. After 48 hours of treatment, the culture medium was discarded and four steps were performed: (1) labeling of the nuclei with DAPI (4', 6-diamidino-2-phenylindole), a fluorescent dye that binds strongly to the adenine rich regions and thymine in DNA sequences (Kim et al., 2012); (2) acquisition of images by inverted fluorescence microscope (Eclipse TE2000-S, Nikon); (3) obtaining the morphometric data (Image Pro Plus program); (4) data analysis (Excel 2013), according to the protocol described by Filippi-Chiela et al. (SPEROTTO, 2014). As a positive control, we have used $150 \mu\text{M}$ hydrogen peroxide (H_2O_2) (Zdanov et al., 2006).

2.10 Quantification of intracellular uridine. Cells were seeded in 24-well plates with cell density of 5×10^4 per well and treated with the selected doses of CPBMF65 and Urd. After 48 hours of treatment, counts were made using tripan blue and each group was adjusted to the amount of 700,000 cells. Cells were washed three times with PBS and disrupted by sonication. The intracellular uridine was then quantified through the High Performance Liquid Chromatography Diode Array Detector (Thermo Scientific). Calibration curve was performed from 0.625 to $20 \mu\text{M}$ with uridine standard (Sigma-Aldrich) and centrifuged at 13000 rpm for 30 min in Amicon microtubes (3 kDa molecular weight cutoff). The samples ($100 \mu\text{l}$) were

injected onto a Sephasil Peptide C18 ST 250 x 4.6 mm, 5 μm , 100 \AA column (GE HealthCare) maintained at 20 $^{\circ}\text{C}$, flow rate set at 0.5 mL/min with a mobile phase of 0.1% Acetic acid. Under these conditions, the retention time of uridine was 31.7 min with a linear relationship ($r > 0.99$) between the peak area and the uridine concentration, normalized by saline group concentration.

2.11 Evaluation of the cell cycle. The FITC BrdU Flow Kit (BD Biosciences, San Jose, CA) was used to evaluate if the treatments would interfere with the cell cycle. HepG2 cells were seeded in 96-well culture plates at a cell density of 2.5×10^4 cells per well. Firstly, cells were "synchronized" for 24 hours and maintained only in culture medium without fetal bovine serum. Afterwards, treatment with the selected doses was performed. After 48 hours of treatment, cells were incubated with BrdU, detached with trypsin and the adjustment was made to the cell suspension containing 1×10^6 cells/ml. Then, samples were fixed with BD Cytotfix/Cytoperm buffer (BD Biosciences). After fixation, cells were treated with Dnase to expose the incorporated BrdU. Subsequently, the total DNA was labeled with 7-AAD. The labeled cells were analyzed on the FACSCanto II flow cytometer (BD Biosciences) and the results analyzed using the program FlowJo 7.6.5 (Tree Star Inc.). As a positive control, hydrogen peroxide (H_2O_2) at the concentration of 150 μM was used.

2.12 Real-time PCR analysis. Approximately 5×10^5 cells were seeded in a 6-well plate, cultured and treated as aforementioned. Total RNA was extracted from cells using Trizol reagent (Invitrogen) according to the manufacturer's instructions. RNA was reverse transcribed into cDNA, using Superscript III First-Strand Synthesis SuperMix (Invitrogen) according to the manufacturer's instructions. Primer sequences used were synthesized by Integrated DNA Technologies (Iowa, USA) with the following sequences: SREBP1c (forward, 5'- CGGAACCATCTTGGCAACAGT-3'; reverse, 5'- CGCTTCTCAATGGCGTTGT-3'; GenBank accession number NM_001005291) and β -actin (forward, 5'- TATGCCAACACAGTGCTGTCTG-3', reverse, 5'- TACTCCTGCTTGCTGATCCACATG-3', GenBank accession number NM_001101.4). The quantity of cDNA was examined by NanoDrop 2000 (Thermo Fisher Scientific). The expression level of SREBP1c and β -actin was quantified by qRT-PCR, which was conducted on Step One Applied Biosystems. The reaction was catalyzed by SYBR Green I (Applied Biosystems- Thermo Fisher Scientific) kit according to the manufacturer's instructions. Data were analyzed with β -actin as a reference gene (control).

2.13 Drug resistance analysis. Cumulative population doubling (CPD) assay was used to evaluate proliferation rate and the regrowth of HepG2 cells after treatment. Approximately

1.2×10^6 cells were seeded and incubated in a 6-well plate for 48 h. After, cells were treated with CPBMF65 90 μM , 180 μM , Urd 10 mM and CDDP 20 μM (positive control) and incubated for 48 h. Control wells received medium and FBS 10%. Cells were harvested and seeded with a cell density of 12×10^4 , 9×10^4 , 6×10^4 and 3×10^4 cells per well in 24-well plates and incubated for 48 h at 37 °C in a 5% CO₂ incubator. Cells were retreated at days 1, 3, 5 and 8, for 48 h, followed by cell counting (Fig.2). Control wells and no retreated wells receive fresh DMEM with 10% FBS in the same time interval. The number of viable cells was determined by mixing 25 μl of cell suspension and 25 μl of 0,4% trypan blue stain solution (Sigma-Aldrich, USA), using a hemocytometer under a light microscope (Nikon Optiphot, Japan). Blue cells were counted as dead cells and the cells that did not absorb were counted as live cells. Cells were counted in the third, fifth, seventh and tenth day after seeded (Lima et al., 2018). PD of each interval was determined according to the formula $PD = [\log N(t) - \log N(t_0)] / \log 2$, where $N(t)$ is the number of cells at the time count, and $N(t_0)$ is the number of cells seeded. The sum of PDs was then plotted against time of culture.

2.14 Statistical analysis. Results were presented through descriptive statistics (mean and standard deviation). For the comparison of means between groups, we have used the one-way analysis of variance (ANOVA) followed by the post-hoc test of Tukey for multiple comparisons. In the presence of asymmetry, the nonparametric correspondent was used. The significance level was set at $p < 0.05$ with a 95% confidence interval and all data were analyzed using SPSS (Statistical Package for Social Sciences) program for Windows, version 15.0. (SPSS Inc. Ohio, USA).

3. RESULTS

3.1 Effect of CPBMF65 on HepG2 cell proliferation, LDH liberation and toxicity in PBMC. Firstly, we have assessed the antiproliferative effect of CPBMF65 at doses of 7.5, 15, 45, 90, 135 and 180 μM in HepG2 cells. Figure 1A shows decreased proliferation at 90, 135 and 180 μM doses. The membrane integrity of CPBMF65-treated HepG2 cells was also analyzed by measuring LDH in the cell supernatant and lysate. Cells were treated with CPBMF65 90, 135 and 180 μM (considering the significant results from our previous experiment) in order to determine its toxicity to cells. There were no significant differences between treatments and control, indicating no significant increase in cell death associated with necrosis in the treated groups as compared to the control group (Fig.1B). We have also treated PBMC with CPBMF65 and analyzed the toxicity using trypan blue. No significant results

were obtained when comparing the treated groups, demonstrating that there was no viability decrease and no toxicity in this primary culture (Fig.1C).

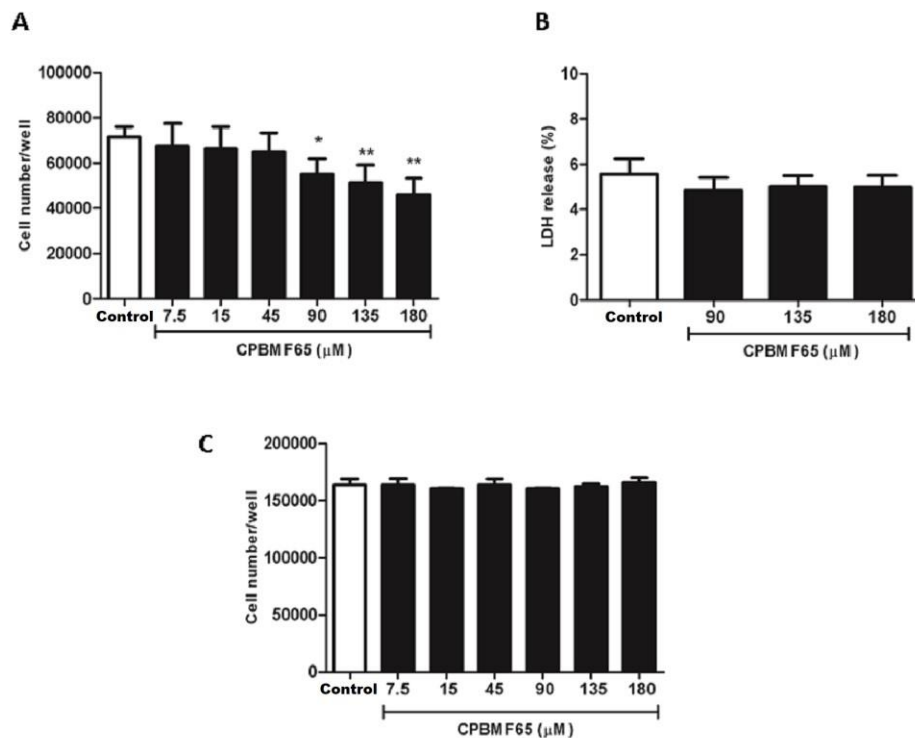


Fig.1 – Effect of CPBMF65 on HepG2 cells proliferation, LDH liberation and toxicity in PBMC: Fig A- HepG2 cells were treated with CPBMF65 (7.5-180 μM) for 48 h and cell number assessed by direct cell count. Data represent the mean \pm SD. Results were expressed as cell number/well. (*, ** $p < 0.05$ vs control, $n=3$). Fig B- Percent of release of lactate dehydrogenase of HepG2 cells after 48 hours of treatment with CPBMF65 90, 135 and 180 μM . Results are expressed as mean \pm SD, $n=3$. Fig C- PBMC were treated with CPBMF65 (7.5-180 μM) for 96 h and cell viability assessed by direct cell count. Data represent the mean \pm SD, $n=3$.

3.2 Effect of CPBMF65 on HepG2 cell Autophagy. Autophagy, a cellular mechanism involving degradation of unnecessary or non-functional components, was analyzed in HepG2 cells through the use of acridine orange dye. We have chosen the 90 μM dose, as it is the lowest dose with a significant antiproliferative effect. The positive control, CDDP 20 μM , was chosen based on previous studies of our laboratory. Cells were quantified using the flow cytometer and visualized under a fluorescent microscope (Fig.2). There was no significant difference between control and CPBMF65 compound. Positive control with Cisplatin (CDDP) had a significant increase of 43%.

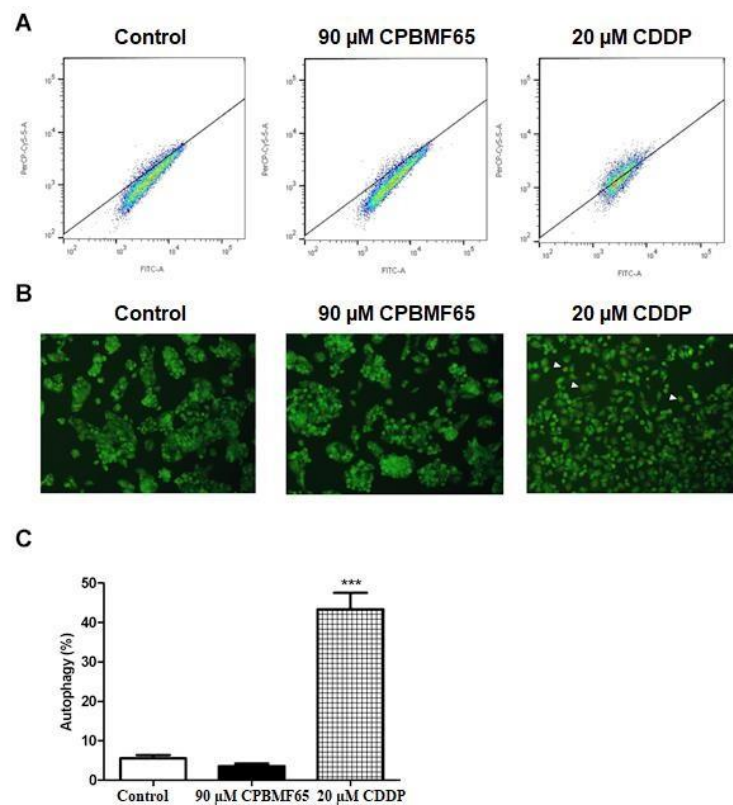


Fig.2 – **Effect of CPBMF65 90 μM and CDDP 20 μM (positive control) on the autophagy of HepG2 cells.** Cells were treated for 48 hours and quantified on the flow cytometer and visualized under a fluorescent microscope. Data presented as mean \pm SD (***) p <0.001 vs control, n=3).

3.3 Effect of CPBMF65 on HepG2 cell apoptosis. In order to verify whether the decrease in proliferation occurred by apoptosis, the PE-Annexin V/7AAD double-labeling assay was used. Once again, the 90 μM concentration was chosen because it is the lowest dose with a significant antiproliferative effect. The positive control, CDDP 40 μM , was chosen based on previous studies of our laboratory. Quantification by flow cytometry showed no significant difference between the CPBMF65-treated and control groups. The CDDP (positive control) had a 45% apoptosis increase (Fig.3).

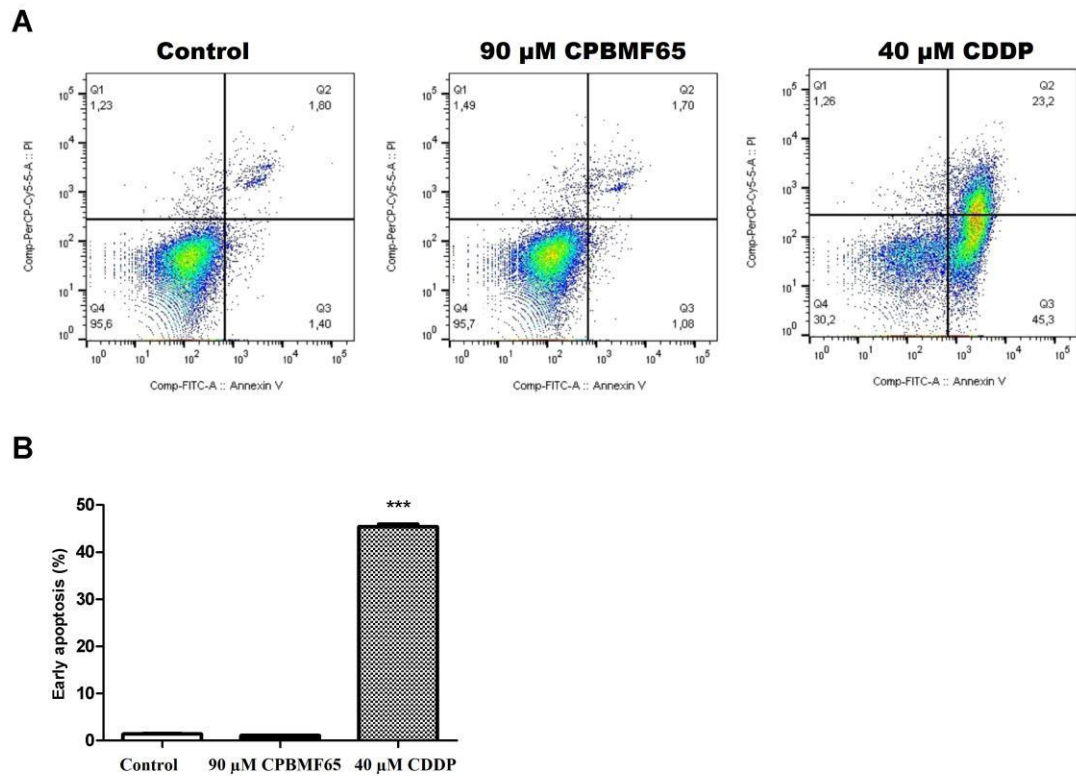


Fig.3 – **Effect of CPBMF65 90 μ M and CDDP 40 μ M (positive control) on the apoptosis of HepG2 cells:** Cells were treated for 48 hours and quantified on the flow cytometer. Data presented as mean \pm SD (***) p <0.001 vs control, n=3).

3.4 Effect of CPBMF65 on oxidative stress. The increase in the production of reactive species of intracellular oxygen can cause cell damage, so we have quantified it by using 2', 7'dichlorofluorescein diacetate (DCFH-DA). The lowest concentration of CPBMF65 resulting in significant antiproliferative effect (90 μ M) was chosen, whereas the positive control, H₂O₂ 1000 μ M, was selected based on previous studies of our laboratory. Control and the groups treated with CPBMF65 presented no significant differences, while the positive control (H₂O₂) showed a significant increase in comparison to the other groups analyzed (Fig.4).

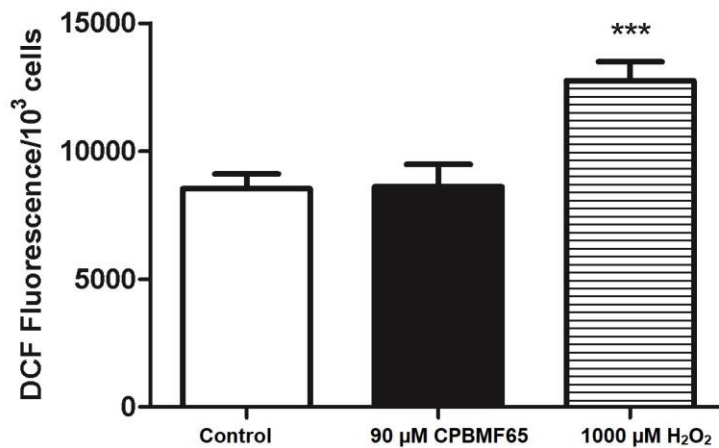


Fig.4 – Effect of CPBMF65 90 µM and H₂O₂ 1000 µM (positive control) on the production of reactive species measured by DCFH-DA: Cells were treated for 48 hours and data presented as mean ± SD (***) $p < 0.001$ vs control, $n=3$).

3.5 Effect of CPBMF65 on HepG2 cell senescence. Another mechanism that may be involved in decreasing cell proliferation is senescence. We have chosen the 90 µM dose as it is the lowest dose with a significant antiproliferative effect. The positive control, H₂O₂ 150 µM, was chosen based on the work of Zdanov et al. (Zdanov et al., 2006). We have observed a 9% senescence increase in HepG2 cells treated with CPBMF65 and 16% in those treated with H₂O₂ (positive control) (Fig.5).

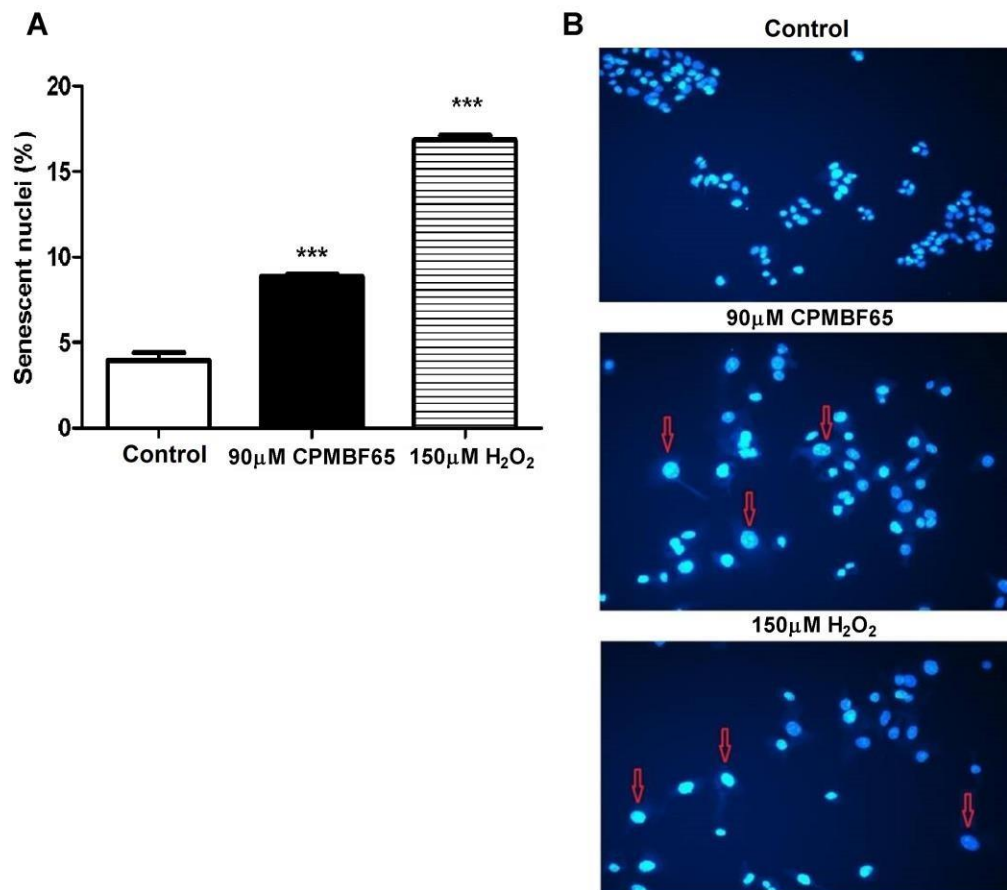


Fig.5 – **Effect of CPBMF65 90 μM and H₂O₂ 150 μM (positive control) on cell senescence:** Cells were treated for 48 hours and data presented as mean ± SD (*** p <0.001 vs control, n=3). The arrows indicate the senescent nuclei.

3.6 Effect of uridine on HepG2 cell proliferation. CPBMF65 is an inhibitor of uridine phosphorylase and considering the possible increase of cellular uridine during the treatment, we have also decided to test the treatment with uridine (Urd) in HepG2 cells. A significant decrease in cell proliferation at 5 and 10 mM Urd was demonstrated (Fig.6). Next, in figure 7, we can verify, through the LDH assay, that these dosages did not show cytotoxicity for HepG2 cells.

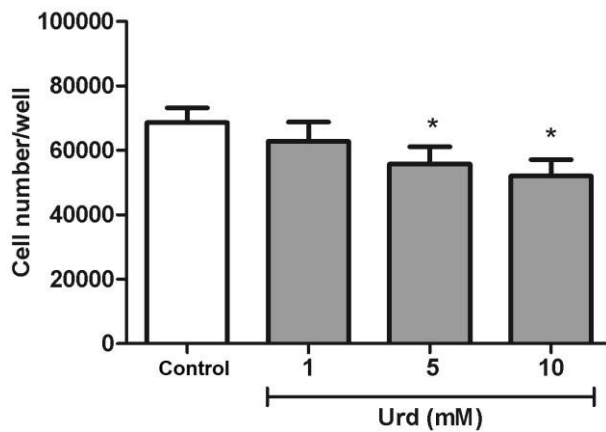


Fig.6 – **Effect of Urd on HepG2 cell proliferation:** Cells were treated with Urd (1, 5, 10 mM) for 48 h and cell viability assessed by direct cell count. Data represent the mean \pm SD. Results were expressed as cell number/well. (* p <0.05 vs control, n=3).

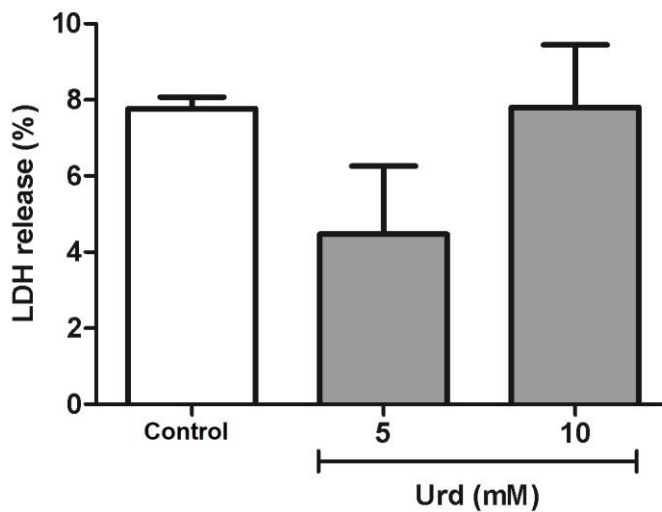


Fig.7 –**Release of lactate dehydrogenase of HepG2 cells:** Cells were treated for 48 hours with Urd 5 and 10 mM. Results are expressed as mean \pm SD, n=3.

3.7. *Effect of uridine on HepG2 cell senescence.* As we obtained a significant increase in senescence with the selected dose of 90 μ M of CPBMF65, we have also performed NMA in the treatment with 5 and 10 mM Urd and H₂O₂ 150 μ M (positive control). We have demonstrated that Urd also provoke increase of senescence in HepG2 cells (Fig.8).

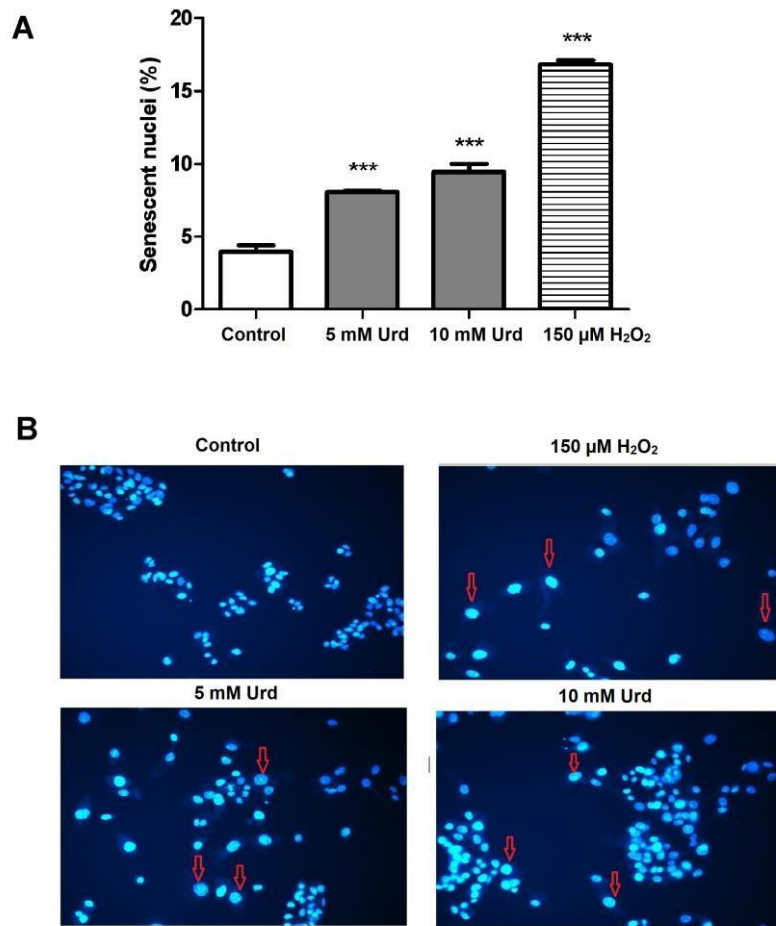


Fig.8 – **Effect of Urd 5 and 10mM and H₂O₂ 150 μM on NMA analyses:** Cells were treated for 48 hours and data presented as mean ± SD (***p*<0.001 vs control, n=3). The arrows indicate the senescent nuclei.

3.8 Evaluation of uridine intracellular on HepG2 cells treated with CPBMF65 and uridine. In order to verify if intracellular Urd may be related to proliferation, we have measured it through HPLC. Results showed, using 700.000 HepG2 cells treated with 90 μM CPBMF65 and Urd 5 and 10 μM, that there is a significant increase of intracellular uridine compared to the control. CPBMF65 also presents significant difference versus Urd 10 mM; and Urd 5 mM versus Urd 10 mM (Fig.9).

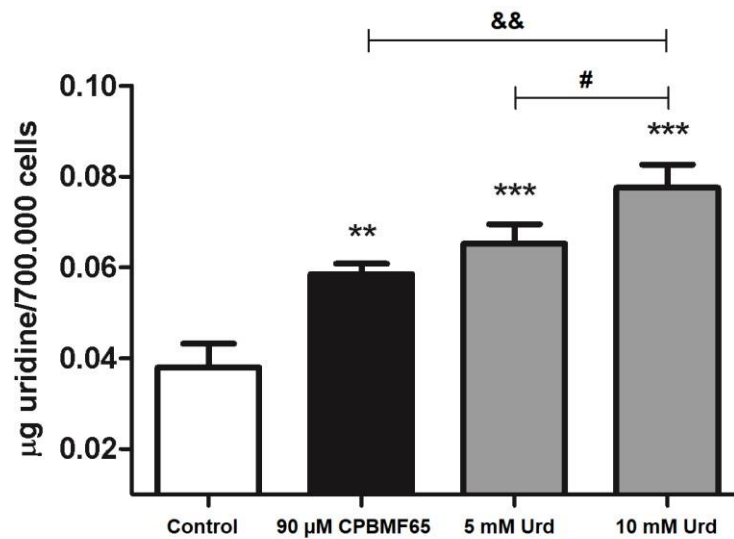


Fig.9 – **Effect of CPBMF65 90 μM and Urd 5 and 10 mM on intracellular Urd:** Cells were treated for 48 hours and data presented as mean ± SD (** $p < 0.05$ and *** $p < 0.001$ vs control, # $p < 0.05$ Urd 5 mM vs Urd 10 mM, && $p < 0.05$ CPBMF65 90 μM vs Urd 10 mM, $n=3$).

3.9 *Impact of CPBMF65 and uridine on HepG2 cells cycle.* After demonstrating a positive result of senescence, we have decided to evaluate the cell cycle stop, so that it can become senescent. In Figure 10 (A and B), for all treatments, we have obtained a significant increase in G0/G1 phase and a decrease in the S and G2/M phases in comparison to the control, which shows that there is a stop of the cell cycle when HepG2 cells are treated with CPBMF65 and Urd.

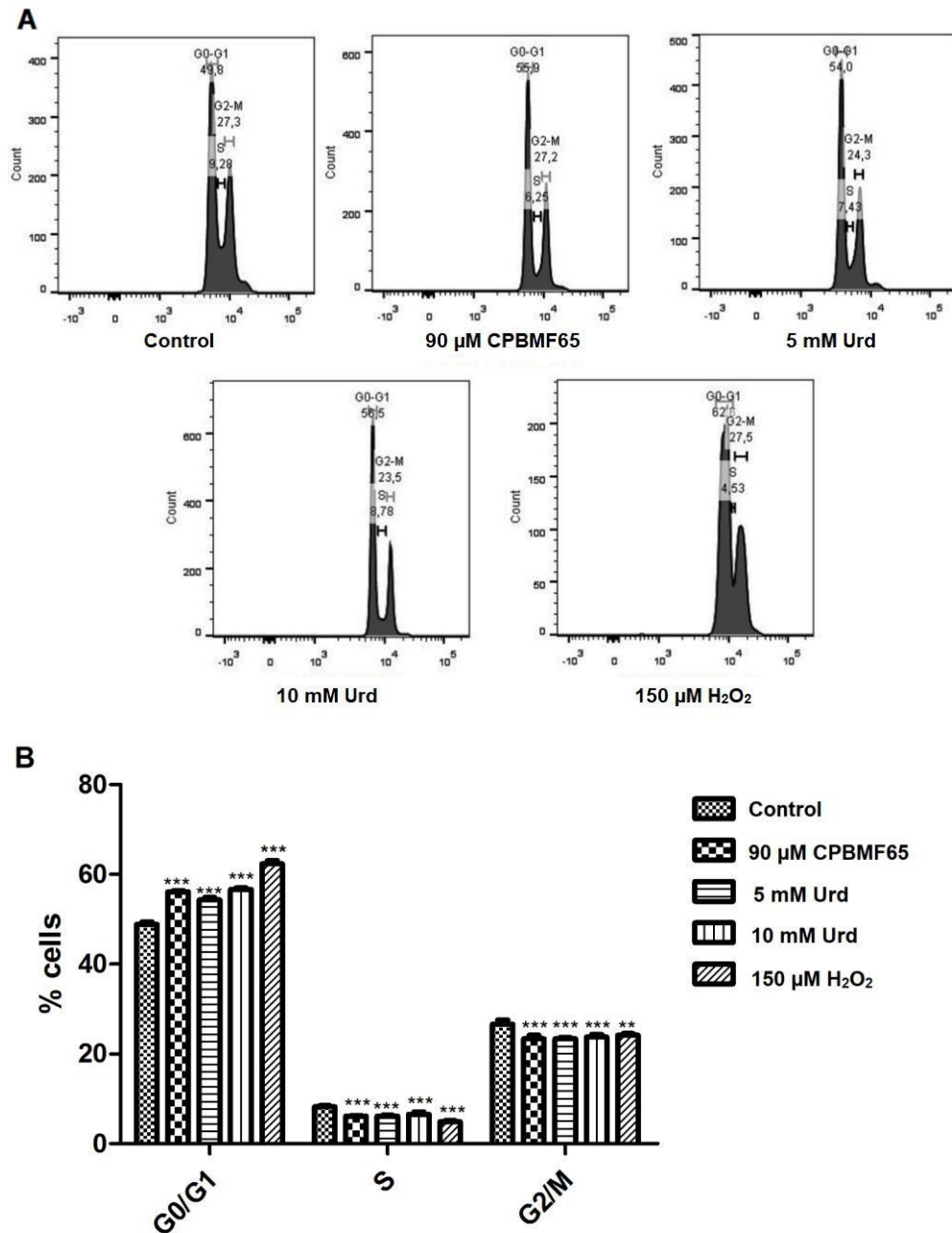


Fig.10 A and B – **Effect of CPBMF65 90 μ M, Urd 5 and 10 mM and H₂O₂ 150 μ M (positive control) on cell cycle:** Cells were treated for 48 hours and data presented as mean \pm SD (***) p <0.001 vs control, n=3).

3.10. Evaluation of p53 expression. The p53 protein is part of the cell cycle arrest and senescence route. Thus, we have analyzed this protein by real-time PCR. The results show that there was an increase of p53 in cells treated with CPBMF65 90 μ M and Urd 10 mM when compared to treatment and control group (fig 11).

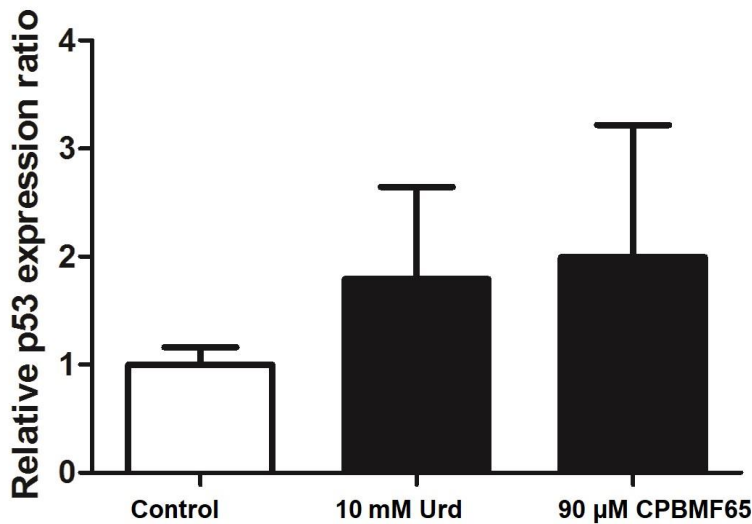


Fig.11 – **Effect of CPBMF65 90 μM and Urd 10 mM on relative p53 expression ratio:** Cells were treated for 48 hours and data presented as mean ± SD, n=3.

3.11 Response of HepG2 cells exposed to long-term treatment with CPBMF65 and

Uridine. we have evaluated the long-term response of HepG2 cells exposed to treatment with CPBMF65 and Urd at the highest doses and we have achieved decreased proliferation in 90 μM, 180 μM CPBMF65 and Urd 10 mM (Fig.12). As a positive control we have used CDDP 20 μM. The treatment with a single dose of CPBMF65 180 μM and the retreatment with 90 μM suppressed the regrowth of HepG2 cells during the period of analysis, as well as the positive control (20 μM CDDP), whereas treatment with CPBMF65 90 μM and 10 mM Urd did not induce this suppression. Besides that, the retreatment with multiple treatment doses of CPBMF65 leads to a stable arrest of the cell growth and a continuous reduction of cell number during the time of analysis, suggesting decreased cell proliferation in agreement with NMA and cell cycle analyzes.

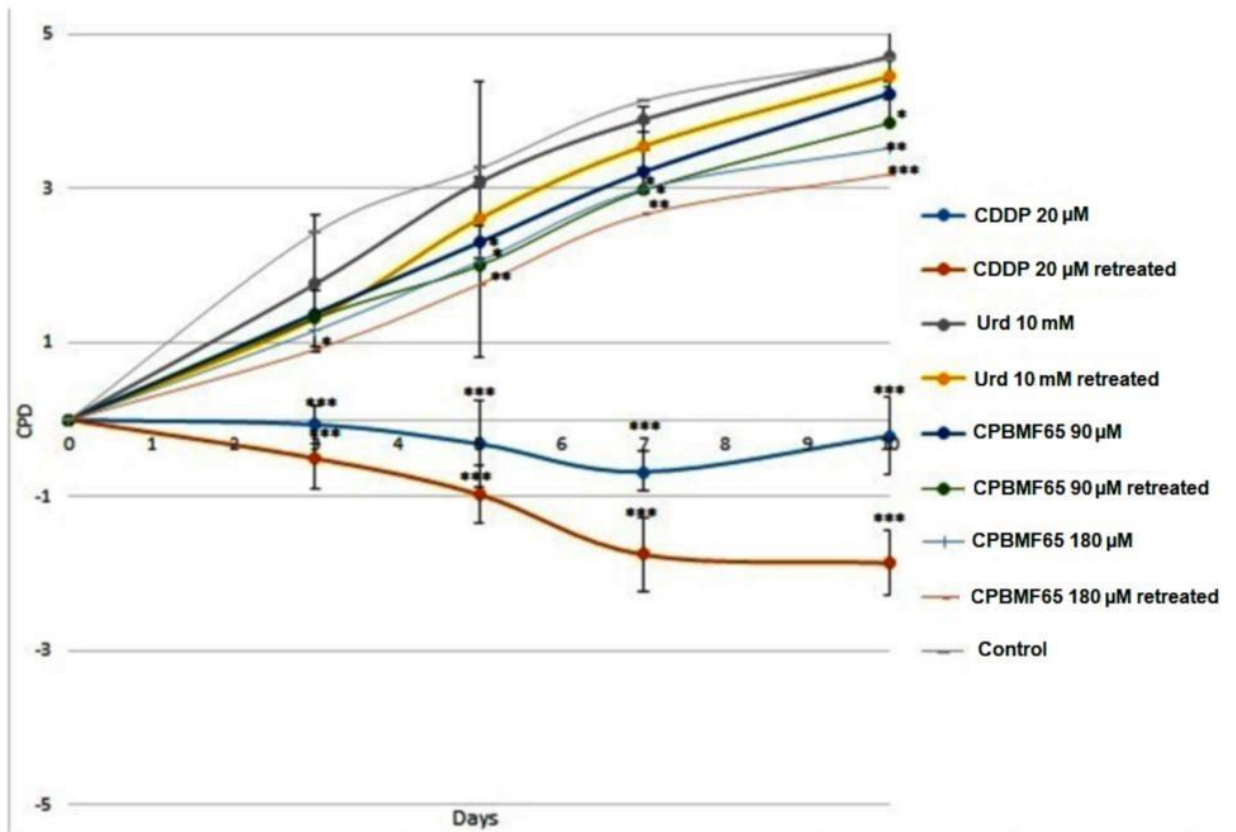


Fig 12 - Effect of CPBMT65 90 and 180 µM, Urd 10 mM and CDDP 20 µM on HepG2 cells regrowth: Data presented as mean ± SD (*, ** $p < 0.05$ and *** $p < 0.001$ vs control, $n=3$). CPD (Cumulative Population Doubling).

4. DISCUSSION

The development of HCC is a process that leads to progressive transformation of normal hepatocytes into highly malignant derivatives. Among them, cell cycle dysregulation is a common feature of human cancer. Therefore, targeting the mitotic phase of the cell cycle may be an effective approach to cancer therapy (Huang et al., 2017). Treatment with CPBMT65, a new molecule that was used for the first time isolated and tested to explore its antiproliferative effects, reduced by 23% the proliferation at a dose of 90 µM in HepG2 cells when compared to control.

Reduction of proliferation in HepG2 cells may be caused by necrosis (cytotoxicity), autophagy, apoptosis, cell cycle arrest or senescence. Therefore, aiming to demonstrate that this effect was not due to necrosis cytotoxicity, we have measured LDH, which did not demonstrate correlation between the ceasing of cell proliferation and death due to necrosis in HepG2 cells.

We have also used trypan blue, which demonstrated absence of necrosis in non-tumoral PBMC. When a tumor is already established, autophagy helps the tumor to survive and grow. However, in the beginning of this process, autophagy can phagocytize the mutated cells and suppress the tumor by isolating damaged organelles, allowing cell differentiation, increasing and promoting cancerous cell death. It may be related to senescence or apoptosis, considering that while autophagy decreases, apoptosis and/or senescence increases (da Silva et al., 2016). Our results show exactly this, a tendency in the reduction of autophagy in comparison to the negative control and a significant increase of the senescence, demonstrated by the NMA analyses. When cells are exposed to mild stress, in cell cycle arrest, growth inhibition and DNA repair may be induced. This response enables cells to restore the damage induced by the cellular stress. However, when cells receive a greater stress stimulus that cannot be controlled, it can result in apoptosis or senescence, the main routes that limit the growth of tumors, preventing proliferation of defective cells (Suzuki and Matsubara, 2011). Our results showed both cell cycle arrest and senescence, demonstrating the evolution of cell arrest to an irreversible mode of cell proliferation.

Oxidative stress usually results from excessive ROS production, mitochondrial dysfunction, impaired antioxidant system, or a combination of these factors. The excessiveness of ROS causes oxidative damage to deoxyribonucleic acid (DNA), proteins, and lipids. ROS can react with nucleic acids attacking nitrogenous bases and sugar phosphate backbone and evoke single and double-stranded DNA breaks (Nita and Grzybowski, 2016). Our results show no significant ROS increase, which may mean that the decrease in proliferation does not occur by this way.

CPBMF65 is an inhibitor of uridine phosphorylase, which creates the possibility of increased intracellular uridine during treatment. This means that when we increase intracellular Urd, it is possible to reduce cancer cell proliferation, because this increase reflects the partial halt of the salvage pathway. The salvage pathway operates to recover bases and nucleosides generated from the breakdown of DNA and RNA. The salvaged bases can be then transformed into nucleotides and reincorporated into DNA. Nucleotides and nucleosides are regenerated and that can contribute to DNA formation, thus reactivating cell proliferation and growth (Squadrito et al., 2017). Thus, accumulation of intracellular urine may help to decrease the proliferation of HepG2 cells. In our results, we found that treatment with Urd did not induce necrosis and reduced the proliferation through the same mechanism demonstrated for CPBMF65 (cell cycle arrest and senescence) in HepG2 cells. In addition, we have measured intracellular Urd and observed that the significant increase in intracellular Urd may

be related to the reduction of HepG2 cellular proliferation. Moreover, we have compared intracellular levels of Urd in HepG2 cells treated with CPBMF65 and Urd, and is interesting that, despite the significant difference between CPBMF65 90 μ M and Urd 10 mM, CPBMF65 increased intracellular Urd with a much lower dose, in μ M, while we had to use Urd in mM to reach a similar result of intracellular uridine increase.

In order to demonstrate that Uridine and CPBMF65 can interfere in the p53 route, we have performed a real-time PCR assay. As the results show, Urd and CPBMF65 can increase the relative p53 expression, although results were not significant. This can be explained considering that in senescence, during the replicative phase, p53 are transiently elevated. p53 initiates the growth arrest, but not appear to entail a consistent, sustained rise levels (Itahana et al., 2001).

We have also assessed cell viability during a longer period with or without retreatment with CPBMF65, Urd and CDDP (positive control). This experiment enabled us to verify a possible long-term regrowth of tumor cells after treatments. The CPBMF65 molecule demonstrated an interesting result maintaining the Cumulative Population Doubling (CPD) reduced during the long-term treatment with a single dose of CPBMF65 180 μ M. CPBMF65 90 μ M also reduced cell proliferation, but only when retreated. However, cells that received treatment with Urd were not able to maintain CPD levels low resulting in proliferation again. The positive control demonstrated with confidence that the technique was successful.

Our results show that CPBMF65 can arrest cell cycle, increase senescence and intracellular Urd in HepG2 cells and have an antiproliferative effect with a long-term response. Treatment with Urd also shows antiproliferative effects, with cell cycle arrest and senescence and increase of intracellular Urd, but it is not able to maintain cell proliferation reduced, even after retreatment. Based on its antitumor activity and low toxicity in normal cells, the new compound, CPBMF65, could be considered a candidate for further research, targeting the identification of new drugs for the treatment of HCC, highlighting the importance of our study by demonstrating its anticancer effects and its use isolated for the first time.

Transparency document

The transparency document associated to this article can be found, in online version.

Acknowledgments

The authors are grateful to G. O. Petersen for his help in the HPLC experiments.

Conflict of interest statement

The authors declare no conflict of interest.

REFERENCE LIST

- Chiela, E.C.F., Protocol for measuring autophagy. <http://www.ufrgs.br/labsinal/autofagia.htm>. (Accessed August 03, 2018).
- da Silva, E.F., Krause, G.C., Lima, K.G., Haute, G.V., Pedrazza, L., Mesquita, F.C., Basso, B.S., Velasquez, A.C., Nunes, F.B., de Oliveira, J.R., 2016. Rapamycin and fructose-1,6-bisphosphate reduce the HEPG2 cell proliferation via increase of free radicals and apoptosis. *Oncol Rep* 36, 2647-2652.
- Huang, R., Xue, R., Qu, D., Yin, J., Shen, X.Z., 2017. Prp19 Arrests Cell Cycle via Cdc5L in Hepatocellular Carcinoma Cells. *Int J Mol Sci* 18.
- Itahana, K., Dimri, G., Campisi, J., 2001. Regulation of cellular senescence by p53. *Eur J Biochem* 268, 2784-2791.
- James, A., Wang, Y., Raje, H., Rosby, R., DiMario, P., 2014. Nucleolar stress with and without p53. *Nucleus* 5, 402-426.
- Khan, F.Z., Perumpail, R.B., Wong, R.J., Ahmed, A., 2015. Advances in hepatocellular carcinoma: Nonalcoholic steatohepatitis-related hepatocellular carcinoma. *World J Hepatol* 7, 2155-2161.
- Kim, T.M., Shin, S.K., Kim, T.W., Youm, S.Y., Kim, D.J., Ahn, B., 2012. Elm tree bark extract inhibits HepG2 hepatic cancer cell growth via pro-apoptotic activity. *J Vet Sci* 13, 7-13.
- Lima, K.G., Krause, G.C., da Silva, E.F.G., Xavier, L.L., Martins, L.A.M., Alice, L.M., da Luz, L.B., Gassen, R.B., Filippi-Chiela, E.C., Haute, G.V., Garcia, M.C.R., Funchal, G.A., Pedrazza, L., Reghelin, C.K., de Oliveira, J.R., 2018. Octyl gallate reduces ATP levels and Ki67 expression leading HepG2 cells to cell cycle arrest and mitochondria-mediated apoptosis. *Toxicol In Vitro* 48, 11-25.
- Nita, M., Grzybowski, A., 2016. The Role of the Reactive Oxygen Species and Oxidative Stress in the Pathomechanism of the Age-Related Ocular Diseases and Other Pathologies of the Anterior and Posterior Eye Segments in Adults. *Oxid Med Cell Longev* 2016, 3164734.
- Pizzorno, G., Cao, D., Leffert, J.J., Russell, R.L., Zhang, D., Handschumacher, R.E., 2002. Homeostatic control of uridine and the role of uridine phosphorylase: a biological and clinical update. *Biochim Biophys Acta* 1587, 133-144.
- Renck, D., Machado, P., Souto, A.A., Rosado, L.A., Erig, T., Campos, M.M., Farias, C.B., Roesler, R., Timmers, L.F., de Souza, O.N., Santos, D.S., Basso, L.A., 2013. Design of novel potent inhibitors of human uridine phosphorylase-1: synthesis, inhibition studies, thermodynamics, and in vitro influence on 5-fluorouracil cytotoxicity. *J Med Chem* 56, 8892-8902.
- Renck, D., Santos, A.A., Jr., Machado, P., Petersen, G.O., Lopes, T.G., Santos, D.S., Campos, M.M., Basso, L.A., 2014. Human uridine phosphorylase-1 inhibitors: a new approach to ameliorate 5fluorouracil-induced intestinal mucositis. *Invest New Drugs* 32, 1301-1307.
- Sachdeva, M., Chawla, Y.K., Arora, S.K., 2015. Immunology of hepatocellular carcinoma. *World J Hepatol* 7, 2080-2090.
- Sperotto, 2014. Protocolos e métodos de análise em laboratórios de biotecnologia agroalimentar e de saúde humana, 1 ed. www.univates.br/editoraunivates/media/publicacoes/74/pdf_74.pdf. (Accessed 27/10 2015).

- Squadrito, F., Bitto, A., Irrera, N., Pizzino, G., Pallio, G., Minutoli, L., Altavilla, D., 2017. Pharmacological Activity and Clinical Use of PDRN. *Front Pharmacol* 8, 224.
- Suzuki, K., Matsubara, H., 2011. Recent advances in p53 research and cancer treatment. *J Biomed Biotechnol* 2011, 978312.
- Yan, R., Wan, L., Pizzorno, G., Cao, D., 2006. Uridine phosphorylase in breast cancer: a new prognostic factor? *Front Biosci* 11, 2759-2766.
- Zdanov, S., Remacle, J., Toussaint, O., 2006. Establishment of H₂O₂-induced premature senescence in human fibroblasts concomitant with increased cellular production of H₂O₂. *Ann N Y Acad Sci* 1067, 210-216.
- Zhang, D., Cao, D., Russell, R., Pizzorno, G., 2001. p53-dependent suppression of uridine phosphorylase gene expression through direct promoter interaction. *Cancer Res* 61, 6899-6905.

Capítulo 4

CONSIDERAÇÕES FINAIS

REFERÊNCIAS

ANEXO- Carta da Comissão de Ética para o Uso de Animais

CONSIDERAÇÕES FINAIS

Fibrose é definida como um processo de cicatrização excessiva que pode gerar danos severos nos tecidos, contribuindo para uma variedade de patologias tais como cirrose e HCC. Não há um tratamento padrão para fibrose hepática, mas alguns estudos já revelaram alvos para prevenir a progressão da fibrose (36). Tradicionalmente, a fibrose hepática é tratada como um processo irreversível, porém estudos recentes apontam novas terapias que resultaram em uma significativa regressão da fibrose hepática (37). O desenvolvimento de HCC é um processo que leva a transformação progressiva de hepatócitos normais a derivados altamente malignos (38). No HCC a desregulação do ciclo celular é um fator comum ao câncer. Portanto, terapias que tem como alvo a fase mitótica do ciclo celular podem ser uma possibilidade para o tratamento e possível regressão do câncer (38). O tratamento com CPBMF65, uma nova molécula usada pela primeira para explorar seus efeitos antiproliferativos em células GRX, HepG2 e linfócitos humanos, reduziu a proliferação celular nos modelos testados e não demonstrou citotoxicidade.

Células hepáticas estreladas (HSC) armazenam vitamina A através de gotas de lipídio. Na presença de lesão hepática, HSC adquirem um fenótipo de ativado, caracterizado por uma expressão elevada de EMC, produção de colágeno I e fibras α -SMA, associadas à perda de gotas lipídicas (39). Nossos resultados demonstraram um aumento significativo das gotas lipídicas evidenciadas pela coloração de ORO, seguida por um aumento significativo da senescência, demonstrado pelas análises de NMA e redução da contração avaliada pelo ensaio de gel de colágeno em grupos tratados das células GRX.

A senescência das HSC ativadas limita a resposta fibrótica aos danos teciduais pela parada do ciclo celular, reduzindo as secreções dos componentes da EMC, aumentando a secreção de enzimas degradantes da EMC e melhorando a resposta imune (40). As gotas lipídicas são abundantes e ampliadas em células senescentes e células tratadas por lipídios específicos tem indução de senescência (41). A desativação de HSC é um alvo importante, diminuindo a produção de componentes da EMC, resultando na redução da contração celular (42). Conseqüentemente, nós podemos correlacionar o aumento de gotas de lipídio e a diminuição da contração das células com o aumento do percentual da senescência e provavelmente com

redução da proliferação das GRX. O aumento da senescência também foi evidenciado nas células HepG2, interligando os resultados de ambas as linhagens.

Cicko et al. demonstrou que a Urd inibe a inflamação e a fibrose na lesão pulmonar por bleomicina, diminuindo a produção de colágeno (33). CPBMF65 é um inibidor da UPP1, que cria a possibilidade de aumento da Urd intracelular durante o tratamento. Isso significa que quando aumentamos a Urd intracelular, é possível reduzir a proliferação celular, pois esse aumento reflete a parada parcial da via de salvamento. A via de salvamento opera para recuperar bases e nucleosídeos gerados a partir da degradação do DNA e do RNA. As bases recuperadas podem então ser transformadas em nucleotídeos e reincorporadas no DNA. Nucleotídeos e nucleósidos são regenerados e podem contribuir para a formação do DNA, reativando assim a proliferação celular e o crescimento (43). Estudos prévios mostraram relação entre o metabolismo da pirimidinas e das doenças hepáticas e sugerem que a Urd poderia ter um efeito protetor que poderia ser explicado pela redução da sua concentração em doenças hepáticas crônicas (32).

O tratamento com injeções intraperitoneais (i.p.) de CPBMF65 em camundongos machos C57BL/6 em dias alternados mostrou-se seguro para os animais, fato evidenciado pela curva de sobrevivência e pelos testes sorológicos dos parâmetros hepáticos. A fim de prevenir danos hepáticos causados pela fibrose hepática induzida por CCl₄ em camundongos, utilizamos injeções de CPBMF65 2mg/kg i.p. durante o período de tratamento de indução. Os níveis de ALT são elevados pelo aumento da lesão hepática causada pelo tratamento CCl₄ e o aumento da expressão de alpha-actina do músculo liso (α -SMA) e colágeno I mostram que o CCl₄ provocou o aparecimento de fibrose hepática. Ao contrário, o tratamento CPBMF65 demonstrou a diminuição destes níveis, sugerindo um efeito protetor da molécula. A avaliação histológica de lâminas do fígado de animais tratados com a combinação de CCl₄ e CPBMF65 por 10 semanas, mostrou uma diminuição estatisticamente significativa na esteatose vesicular, na inflamação, balonismo hepatocelular e da fibrose, comprovando seu efeito hepatoprotetor.

Considerando resultados deste trabalho, nós acreditamos que o tratamento com CPBMF65 pode reverter o fenótipo ativado de HSC com o aumento de gotas lipídicas, redução da contração e pode reduzir a proliferação das GRX, suportada

provavelmente por um aumento da senescência. CPBMF65 também parece atenuar a inflamação e a fibrose de fígado no modelo animal da toxicidade severa induzida por CCl₄. Por estes motivos nós fizemos a sequência dos estudos da molécula em câncer, utilizando as células HepG2.

No estudo em que utilizamos as células HepG2 como um modelo *in vitro* de câncer hepático, verificamos que a droga provocou uma diminuição significativa na proliferação celular destas células como uma consequência da parada do ciclo e senescência celular, além do aumento intracelular de Urd. Como encontramos aumento da Urd intracelular, também testamos doses de Urd nas células HepG2. Demonstramos que o tratamento com Urd também diminui a proliferação de células HepG2 através da parada do ciclo e senescência celular em tratamentos agudos, porém, não pode manter os baixos níveis de proliferação durante o tratamento crônico. Ao contrário, o tratamento com CPBMF65 mostrou que as células HepG2 permaneceram em baixos níveis proliferativos durante este tratamento prolongado.

Nossas perspectivas futuras são testar os efeitos *in vivo* da CPBMF65 em modelos animais com hepatocarcinoma induzido.

REFERÊNCIAS

1. Poole LG, Arteel GE. Transitional Remodeling of the Hepatic Extracellular Matrix in Alcohol-Induced Liver Injury. *BioMed research international*. 2016;2016:3162670.
2. Lee UE, Friedman SL. Mechanisms of hepatic fibrogenesis. *Best practice & research Clinical gastroenterology*. 2011;25(2):195-206.
3. Hou W, Syn WK. Role of Metabolism in Hepatic Stellate Cell Activation and Fibrogenesis. *Frontiers in cell and developmental biology*. 2018;6:150.
4. Anthony B, Allen JT, Li YS, McManus DP. Hepatic stellate cells and parasite-induced liver fibrosis. *Parasites & vectors*. 2010;3(1):60.
5. Borojevic R, Monteiro AN, Vinhas SA, Domont GB, Mourao PA, Emonard H, et al. Establishment of a continuous cell line from fibrotic schistosomal granulomas in mice livers. *In vitro cellular & developmental biology : journal of the Tissue Culture Association*. 1985;21(7):382-90.
6. Bitencourt S, de Mesquita FC, Caberlon E, da Silva GV, Basso BS, Ferreira GA, et al. Capsaicin induces de-differentiation of activated hepatic stellate cell. *Biochemistry and cell biology = Biochimie et biologie cellulaire*. 2012;90(6):683-90.
7. INCA. Câncer de Fígado 2013 [07.09.2015]. Available from: <http://www2.inca.gov.br/wps/wcm/connect/tiposdecancer/site/home/figado>
8. Khan FZ, Perumpail RB, Wong RJ, Ahmed A. Advances in hepatocellular carcinoma: Nonalcoholic steatohepatitis-related hepatocellular carcinoma. *World J Hepatol*. 2015;7(18):2155-61.
9. Hu Q, Lou GG, Liu YC, Qian L, Lv BD. The Tumor Necrosis Factor-alpha-308 and -238 Polymorphisms and Risk of Hepatocellular Carcinoma for Asian Populations: A Meta-Analysis. *Current therapeutic research, clinical and experimental*. 2014;76:70-5.
10. Sachdeva M, Chawla YK, Arora SK. Immunology of hepatocellular carcinoma. *World J Hepatol*. 2015;7(17):2080-90.
11. Organization WH. The top 10 causes of death. 2014 [03.09.2015]. Available from: <http://www.who.int/mediacentre/factsheets/fs310/en/index.html>.
12. Salhab M, Canelo R. An overview of evidence-based management of hepatocellular carcinoma: a meta-analysis. *Journal of cancer research and therapeutics*. 2011;7(4):463-75.
13. Kew MC. Aflatoxins as a cause of hepatocellular carcinoma. *Journal of gastrointestinal and liver diseases : JGLD*. 2013;22(3):305-10.
14. Magnussen A, Parsi MA. Aflatoxins, hepatocellular carcinoma and public health. *World journal of gastroenterology : WJG*. 2013;19(10):1508-12.
15. Hep G2 [HEPG2] (ATCC® HB-8065™) Available from: <http://www.atcc.org/products/all/HB-8065.aspx>.
16. Wilkening S, Stahl F, Bader A. Comparison of primary human hepatocytes and hepatoma cell line Hepg2 with regard to their biotransformation properties. *Drug metabolism and disposition: the biological fate of chemicals*. 2003;31(8):1035-42.
17. Athwal VS, Pritchett J, Martin K, Llewellyn J, Scott J, Harvey E, et al. SOX9 regulated matrix proteins are increased in patients serum and correlate with severity of liver fibrosis. *Scientific reports*. 2018;8(1):17905.
18. Friedman SL. Mechanisms of hepatic fibrogenesis. *Gastroenterology*. 2008;134(6):1655-69.
19. Hocayen PA, Grassioli S, Leite NC, Pochapski MT, Pereira RA, da Silva LA, et al. *Baccharis dracunculifolia* methanol extract enhances glucose-stimulated insulin

- secretion in pancreatic islets of monosodium glutamate induced-obesity model rats. *Pharmaceutical biology*. 2015;1-9.
20. Vargha R, Mostafa G, Burda G, Hermon M, Trittenwein G, Golej J. Treatment with N-Acetylcystein and Total Plasma Exchange for Extracorporeal Liver Support in Children with Paracetamol Intoxication. *Klinische Padiatrie*. 2014.
 21. Galicia-Moreno M, Rodriguez-Rivera A, Reyes-Gordillo K, Segovia J, Shibayama M, Tsutsumi V, et al. N-acetylcysteine prevents carbon tetrachloride-induced liver cirrhosis: role of liver transforming growth factor-beta and oxidative stress. *European journal of gastroenterology & hepatology*. 2009;21(8):908-14.
 22. Tao YY, Yan XC, Zhou T, Shen L, Liu ZL, Liu CH. Fuzheng Huayu recipe alleviates hepatic fibrosis via inhibiting TNF-alpha induced hepatocyte apoptosis. *BMC complementary and alternative medicine*. 2014;14:449.
 23. Hempfling W, Dilger K, Beuers U. Systematic review: ursodeoxycholic acid--adverse effects and drug interactions. *Alimentary pharmacology & therapeutics*. 2003;18(10):963-72.
 24. Vargas-Mendoza N, Madrigal-Santillan E, Morales-Gonzalez A, Esquivel-Soto J, Esquivel-Chirino C, Garcia-Luna YG-RM, et al. Hepatoprotective effect of silymarin. *World J Hepatol*. 2014;6(3):144-9.
 25. Freitag AF, Cardia GF, da Rocha BA, Aguiar RP, Silva-Comar FM, Spironello RA, et al. Hepatoprotective Effect of Silymarin (*Silybum marianum*) on Hepatotoxicity Induced by Acetaminophen in Spontaneously Hypertensive Rats. *Evidence-based complementary and alternative medicine : eCAM*. 2015;2015:538317.
 26. Attwa MH, El-Etreby SA. Guide for diagnosis and treatment of hepatocellular carcinoma. *World J Hepatol*. 2015;7(12):1632-51.
 27. Abbasoglu O. Role of liver resection in the management of multinodular hepatocellular carcinoma. *World J Hepatol*. 2015;7(20):2237-40.
 28. Seber A, Miachon AS, Tanaka ACS, Castro ÂMSe, Carvalho AC, Petrilli AS, et al. I Diretriz brasileira de cardio-oncologia pediátrica da Sociedade Brasileira de Cardiologia. *Arquivos Brasileiros de Cardiologia*. 2013;100:1-68.
 29. Renck D, Machado P, Souto AA, Rosado LA, Erig T, Campos MM, et al. Design of novel potent inhibitors of human uridine phosphorylase-1: synthesis, inhibition studies, thermodynamics, and in vitro influence on 5-fluorouracil cytotoxicity. *Journal of medicinal chemistry*. 2013;56(21):8892-902.
 30. Renck D, Santos AA, Jr., Machado P, Petersen GO, Lopes TG, Santos DS, et al. Human uridine phosphorylase-1 inhibitors: a new approach to ameliorate 5-fluorouracil-induced intestinal mucositis. *Investigational new drugs*. 2014;32(6):1301-7.
 31. Pizzorno G, Cao D, Leffert JJ, Russell RL, Zhang D, Handschumacher RE. Homeostatic control of uridine and the role of uridine phosphorylase: a biological and clinical update. *Biochimica et biophysica acta*. 2002;1587(2-3):133-44.
 32. Schofield Z, Reed MA, Newsome PN, Adams DH, Gunther UL, Lalor PF. Changes in human hepatic metabolism in steatosis and cirrhosis. *World journal of gastroenterology : WJG*. 2017;23(15):2685-95.
 33. Cicko S, Grimm M, Ayata K, Beckert J, Meyer A, Hossfeld M, et al. Uridine supplementation exerts anti-inflammatory and anti-fibrotic effects in an animal model of pulmonary fibrosis. *Respiratory research*. 2015;16:105.
 34. Cao D, Ziemba A, McCabe J, Yan R, Wan L, Kim B, et al. Differential expression of uridine phosphorylase in tumors contributes to an improved fluoropyrimidine therapeutic activity. *Molecular cancer therapeutics*. 2011;10(12):2330-9.

35. Renck D, Ducati RG, Palma MS, Santos DS, Basso LA. The kinetic mechanism of human uridine phosphorylase 1: Towards the development of enzyme inhibitors for cancer chemotherapy. *Archives of biochemistry and biophysics*. 2010;497(1-2):35-42.
36. Bataller R, Brenner DA. Liver fibrosis. *The Journal of clinical investigation*. 2005;115(2):209-18.
37. Povero D, Busletta C, Novo E, di Bonzo LV, Cannito S, Paternostro C, et al. Liver fibrosis: a dynamic and potentially reversible process. *Histology and histopathology*. 2010;25(8):1075-91.
38. Huang R, Xue R, Qu D, Yin J, Shen XZ. Prp19 Arrests Cell Cycle via Cdc5L in Hepatocellular Carcinoma Cells. *International journal of molecular sciences*. 2017;18(4).
39. Bobowski-Gerard M, Zummo FP, Staels B, Lefebvre P, Eeckhoutte J. Retinoids Issued from Hepatic Stellate Cell Lipid Droplet Loss as Potential Signaling Molecules Orchestrating a Multicellular Liver Injury Response. *Cells*. 2018;7(9).
40. Krizhanovsky V, Yon M, Dickins RA, Hearn S, Simon J, Miething C, et al. Senescence of activated stellate cells limits liver fibrosis. *Cell*. 2008;134(4):657-67.
41. Flor AC, Wolfgeher D, Wu D, Kron SJ. A signature of enhanced lipid metabolism, lipid peroxidation and aldehyde stress in therapy-induced senescence. *Cell death discovery*. 2017;3:17075.
42. Basso BS, de Mesquita FC, Dias HB, Krause GC, Scherer M, Santarem ER, et al. Therapeutic effect of *Baccharis anomala* DC. extracts on activated hepatic stellate cells. *EXCLI journal*. 2019;18:91-105.
43. Squadrito F, Bitto A, Irrera N, Pizzino G, Pallio G, Minutoli L, et al. Pharmacological Activity and Clinical Use of PDRN. *Frontiers in pharmacology*. 2017;8:224.

ANEXO- Carta da Comissão de Ética para o Uso de Animais

Esta mensagem foi emitida automaticamente pelo SIPESQ - Sistema de Pesquisas da PUC

Prezado(a) Coordenador(a) de Projeto de Pesquisa,

A **CEUA** considerou que o projeto **7088 - AVALIAÇÃO DA ATIVIDADE ANTINEOPLÁSICA DO COMPOSTO CPBMF65, UM INIBIDOR DA ENZIMA URIDINA FOSFORILASE 1 HUMANA: UM ESTUDO IN VITRO E IN VIVO** atende aos requisitos por ela definidos.

Desta forma, o projeto já pode ser iniciado.

Atenciosamente,

Pró-Reitoria de Pesquisa, Inovação e Desenvolvimento
